

國立臺灣大學醫學院毒理學研究所

博士論文

Graduate Institute of Toxicology

College of Medicine

National Taiwan University

Doctoral Dissertation



眼鏡蛇咬傷致潰爛毒性機轉探討

Approach for the mechanisms of *Naja atra*
snakebite-related dermonecrosis

何政軒

Cheng-Hsuan Ho

指導教授:劉興華 博士

Advisor: Shing-Hwa Liu, Ph.D

中華民國 110 年 12 月

December 2021

國立臺灣大學博士學位論文
口試委員會審定書

眼鏡蛇咬傷致潰爛毒性機轉探討
Approach for the mechanisms of *Naja atra*
snakebite-related dermonecrosis

本論文係何政軒君 (D04447001) 在國立臺灣大學醫學院毒理研究所完成之博士學位論文，於民國 110 年 12 月 9 日承下列考試委員審查通過及口試及格，特此證明

口試委員：

劉興華

(簽名)

藍國徵 (指導教授)

劉興華

(簽名)

姜至剛

(簽名)

許昭芳

(簽名)

蕭水銀

(簽名)

系主任、所長

劉東慧

(簽名)

謝辭



路漫漫其修遠兮

吾將上下而求索


感謝家人: 侯婷婷、何東演、王秋妹、何書安、何佩芹、何沛樵、何佩宸

感謝貴人: 林錦生教授(三軍總醫院心臟血管內科)、毛彥喬主任(台中榮民總醫院毒物科)、江廖峻助理教授(國防醫學院生物及解剖學研究所)、徐志雄助理教授(國防醫學院醫科所博士)

摘要

蛇類咬傷是(亞)熱帶地區重要且特有的疾病。台灣民眾最常被咬傷的三種陸生蛇種，分屬兩科，蝮蛇科(龜殼花與青竹絲)以及眼鏡蛇科(中華眼鏡蛇)。共同臨床症狀為疼痛與持續腫脹，中華眼鏡蛇咬傷的病人有高比例呈現傷口潰爛與組織壞死。台灣抗蛇毒血清成功降低了蛇咬傷病人的死亡率，但臨床研究發現血清似乎無法立即改善進展性腫脹或傷口潰爛，因此何時需要手術介入，一直是臨床決策困擾之處。隨著研究發現，使用超音波監測模組可以判斷蛇咬傷後進展性腫脹是否產生急性腔室症候群，臨床醫師依據結果建議病人是否需要接受筋膜切開術。然而眼鏡蛇咬傷後傷口潰爛的機轉與血清中和效果仍是待釐清的問題。推測此潰爛機轉可能為蛇毒引發的免疫反應與毒素組織破壞作用的兩者共同效果。先前研究發現黑頸眼鏡蛇蛇毒會吸引嗜中性球參與免疫反應；蛇毒成分中的細胞毒素，磷脂酶 A2，及蛇毒金屬蛋白酶也具有破壞組織作用。本研究目標在探討中華眼鏡蛇蛇毒造成皮膚組織潰爛的機轉，分析蛇毒粗毒是否誘發嗜中性球胞外陷阱的免疫反應，使用細胞毒性方式分析毒素中主要致潰爛成分，同時評估現行使用血清中和潰爛的有效性。

首先利用不同溶解度與滲透度的特性，分離出健康成年人之嗜中性白血球，使用中華眼鏡蛇的不同粗毒濃度刺激 180 分鐘，西方墨點法定量第四型蛋白精氨酸脫亞氨酶和第三型瓜氨酸化組織蛋白，隨著粗毒濃度上升會誘發嗜中性球胞外陷阱反應。有別於以半數致死劑量與存活率討論血清的有效性，本研究採用世界衛生組織建議的最小致潰爛劑量方式做細胞毒性評估，來確立中華眼鏡蛇毒粗毒中何者為主要致潰爛毒素且評估血清的中和效果。然而使用中華眼鏡蛇粗毒進行動物潰爛評估測時，動物會死亡而未出現傷口潰爛。因此本研究先移除中華眼鏡蛇毒中對於動物的致命毒素，神經毒素，再以不同濃度注射於小鼠背部皮內，三天後，測量潰爛面積是否達直徑 5 毫米，實驗結果最小致潰爛濃度為 0.494 ± 0.029 $\mu\text{g/g}$ 。以組織切片的方式觀察潰爛進展，越深層的皮膚，潰爛情形越嚴重。再依序去除其他主要毒素成分，釐清主要致潰爛成分為細胞毒素。最後以不同稀釋倍數血清與挑戰劑量(兩倍最小致潰爛濃度)蛇毒混合後，打入小鼠背部皮膚，三天後，不論何種稀釋倍數，相比於挑戰劑量造成的潰爛直徑，均無法使其減少一半以上。

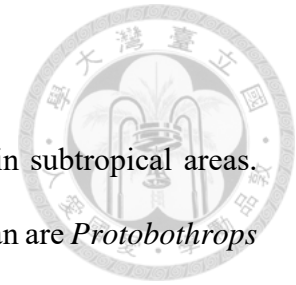


蛇毒誘發嗜中性球胞外陷阱後，蛇毒毒素被胞外陷阱圈住，阻止擴散反而提高局部環境的毒素濃度，附著於胞外陷阱網狀骨架上的蛋白酶，也會造成局部組織破壞。研究指出破壞胞外陷阱結構，可以減少毒素與蛋白酶對組織破壞但卻使毒素散布，反而會降低小鼠存活率。因此為了避免蛇咬傷後傷口組織潰爛而破壞胞外陷阱結構，整體效益仍有待評估。至於不同蛇種產生的胞外陷阱現象，過往研究有不同的結果。歸納而言，蝮蛇科與眼鏡蛇科誘發嗜中性球胞外陷阱機轉不同，蝮蛇科可能為自殺性胞外陷阱，需要刺激一段時間後才會出現，且隨刺激濃度增高而反應增加；眼鏡蛇科則為存活性胞外陷阱，可以短時間內出現。本研究的結果與先前其他種類眼鏡蛇的結果相似，嗜中性球胞外陷阱反應會在毒素刺激後短時間內產生，隨著毒素濃度上升但是高濃度時會減少。中華眼鏡蛇有別於黑頸眼鏡蛇，有較多的神經毒素成分，中華眼鏡蛇需先移除神經毒素才能在動物模式上觀察到傷口潰爛變化。病人被中華眼鏡蛇咬傷後幾乎無神經症狀，表示神經毒素在人體似乎作用不大，因此移除神經毒素後探討傷口變化的動物模式更貼近臨床狀況。台灣抗蛇毒血清抗體計量為田中單位，以往由動物實驗獲得半數致死劑量再求得半數有效劑量，進而推估建議的血清施打劑量。近年學者建議根據臨床症狀來調整施打劑量。然而根據本研究，現行血清並無法中和中華眼鏡蛇致潰爛效果。

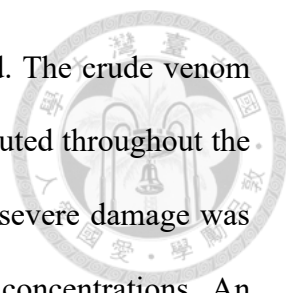
本研究釐清了中華眼鏡蛇的粗毒會引起嗜中性球胞外陷阱，主要致潰爛成分為細胞毒素。毒素引發嗜中性球胞外陷阱的免疫反應與細胞毒素的破壞作用，兩者協同結果造成中華眼鏡蛇咬傷後潰爛變化，且現行血清並無中和中華眼鏡蛇毒致潰爛的效果。展望未來，中華眼鏡蛇咬傷的病人除了接受現行血清以減少系統性毒素，也許還要合併其他輔助治療，如對細胞毒素的單株抗體，或是有效的除汙治療。

關鍵字:中華眼鏡蛇，急性腔室症候群，超音波，最小致潰爛濃度，細胞毒素，嗜中性球胞外陷阱。

Abstract



Snakebite envenomation is an important and neglected issue in subtropical areas. The most frequently encountered species causing snakebites in Taiwan are *Protobothrops mucrosquamatus*, *Trimeresurus stejnegeri* (family: Viperidae) and *Naja atra* (family: Elapidae). Snakebite envenomation includes systemic toxicities and local injuries. In clinical practice, antivenom indeed ameliorates snakebite-induced systemic toxicity; however, it seems to exert few effects on local injuries, including progressive swelling and dermonecrosis. Intervention with the protocol of point-of-care ultrasound (POCUS) may facilitate clinical decisions for snakebite envenomation, especially acute compartment-like syndrome. Indirect tissue injury caused by immune reactions, such as neutrophil extracellular traps (NETs) triggered by snakebite envenomation and the direct effects of different components of venom, are possible mechanisms of dermonecrosis. The AIM of this study is to evaluate the mechanism of *N. atra* snakebite-related dermonecrosis via the formation of NETs and to clarify the major component of venom. Neutrophils isolated from healthy adults were mixed with different levels of crude *N. atra* venom for 180 minutes, and then NET formation was analyzed by performing a western blot analysis of PAD₄ and H₃Cit. Neurotoxins (NTXs) were removed from crude venom (deNTXs), and different concentrations of deNTXs were injected intradermally into the dorsal skin of mice. After three days, the minimum necrotizing dose (MND) was calculated. The mice were injected with a challenge dose (two times the MND) mixed with different dilutions of antivenom (from the original concentration to a 1:5 dilution) and compared with the challenge dose mixed with saline. A reduction in the necrotic diameter of 50% was used to identify the MND₅₀. Furthermore, both phospholipase A₂ (PLA₂) and cytotoxins (CTXs) were separately removed from the deNTXs to identify the



major necrosis-inducing factor, and the necrotic lesions were scored. The crude venom of *N. atra* induced the formation of NETs. The deNTXs were distributed throughout the soft tissue rather than remaining localized at the injection site, and severe damage was observed in the panniculus carnosus and adventitia, even at low concentrations. An evaluation of the neutralizing ability of antivenom on the LD₅₀ in mice alone is not adequate to assess necrosis. The MND of the deNTXs for mice was 0.494 ± 0.029 µg/g. Regardless of the concentration of antivenom, including the original concentration, the challenge dose of deNTXs resulted in necrosis throughout all layers of the skin. Antivenom was ineffective at preventing necrosis. *N. atra* snakebite-related dermonecrosis may be attributed to venom-induced NET formation and the effect of CTXs. CTXs play a major role in *N. atra*-related necrosis. The deNTX animal model is suitable for assessing *N. atra*-related dermonecrosis. In the future, management of *N. atra* bites may include not only the existing antivenom to improve the survival rate but also the administration of monoclonal antibodies against CTXs or combined treatment with other therapies.

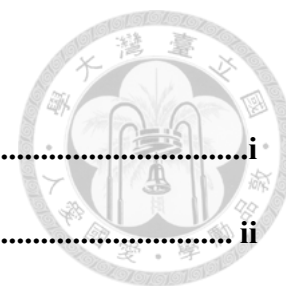
Keywords: *Naja atra*, Snakebite, Taiwan, point-of-care ultrasound, acute compartment syndrome, minimum necrotizing dose, neurotoxin, cytotoxin, neutrophil extracellular trap



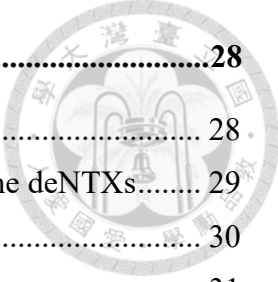
Abbreviation

ACS	Acute compartment syndrome
CTXs	Cytotoxins, also called cardiotoxins
DRAF	Diastolic retrograde arterial flow
deNTXs	Crude venom of <i>Naja atra</i> with the removal of neurotoxins
ED 50	50% effective dose
H3Cit	Citrullinated histone H3
HBSS (-)	Hanks' Balanced Salt Solution without Ca, Mg, or phenol red
HMWP	High-molecular-weight proteins
IP	Intracompartmental pressure
LAAO	L-amino acid oxidase
LD 50	50% lethal dose
MMPs	Matrix metalloproteinase metalloproteinases
MND	minimum necrotizing dose
MPO	Myeloperoxidase
NETs	Neutrophil extracellular traps
NTXs	Neurotoxins, also known as cobrotoxin
PAD4	Protein-arginine deiminase type 4
PLA2	Phospholipase A2
PMA	Phorbol 12 myristate 13 acetate
POCUS	Protocol of point-of-care ultrasound
SCE	Subcutaneous edema
SVMPs	Snake venom metalloproteinases

Contents



謝辭	i
摘要	ii
Abstract	iv
Abbreviation	vi
Contents	vii
Chapter 1 Introduction	1
1-1 Snake classification and regional distribution in Taiwan	1
1-2 Clinical presentation of snakebite	2
1-3 Pathogenesis of snakebite-related dermonecrosis	5
1-3-1 Progression of dermonecrosis	5
1-3-2 Neutrophil reaction	5
1-4 Features of venom	8
1-4-1 SVMs, snake venom metalloproteinases	8
1-4-2 PLA ₂ , phospholipase A ₂	9
1-4-3 CTXs, cytotoxins (also called cardiotoxins)	10
1-5 Evaluation of the venom-induced cytotoxic effect	11
1-6 AIM	12
Chapter 2 Materials and Methods	13
2-1 Patient recruitment	13
2-2 Animals	15
2-3 Human neutrophil isolation	16
2-4 Western blot analysis of snake venom-induced NET formation	18
2-5 Chemicals and reagents	19
2-6 Snake Venom Approach and Analysis	20
2-7 Preparation of deNTXs, deNTXs-deCTXs, and deNTXs-dePLA ₂	21
2-8 Minimum Necrotizing Dose (MND)	22
2-9 MND50: Efficacy of Antivenom Neutralization	23
2-10 Biopsy and Necrosis Score	24
2-11 Point-of-care ultrasound (POCUS)	25
2-12 data analysis	27



Chapter 3 Results	28
3-1 Crude <i>N. atra</i> venom induces NET formation	28
3-2 Characterization of <i>Naja atra</i> Crude Venom and the MND of the deNTXs.....	29
3-3 CTXs are the Major Component Causing Necrosis	30
3-4 Development of Necrosis	31
3-5 Neutralization Ability of the Antivenom.....	32
Chapter 4 Discussion.....	33
Chapter 5 Conclusions	40
Chapter 6 Future perspectives	41
Chapter 7 List of publications	42
References	65

List of Figures

Figure 1 <i>Protobothrops mucrosquamatus</i> and <i>Naja atra</i>	43
Figure 2 <i>Protobothrops mucrosquamatus</i> related progress proximal edema	44
Figure 3 <i>Protobothrops mucrosquamatus</i> related dermonecrosis	45
Figure 4 Point-of-care ultrasound (POCUS)	46
Figure 5 <i>Naja atra</i> dermonecrosis	47
Figure 6 Neutrophil and Neutrophil extracellular trap	48
Figure 7 Western blot analysis of <i>Naja atra</i> related NET	49
Figure 8 Characterization of <i>Naja atra</i> crude venom and crude venom devoid of NTXs.	50
Figure 9 Intradermal injection with deNTXs <i>N. atra</i> venom	51
Figure 10 Minimal necrosis dose of different component of venom	52
Figure 11 Skin biopsy of different levels of deNTXs <i>N. atra</i> venom	53
Figure 12 Tissue necrosis score of different levels of deNTXs <i>N. atra</i> venom	54
Figure 13 Skin biopsy of different dilutions of antivenom mixed with challenge dose	55
Figure 14 Tissue necrosis score of different dilutions of antivenom mixed with challenge dose	56
Figure 15 Graphical abstract	57

List of Tables

Table 1 Major species of venomous snakes in Taiwan.....	58
Table 2 Minimum necrotizing dose (MND) in different components of <i>Naja atra</i> .	59
Table 3 Tissue necrosis score	60
Table 4 Necrosis scores with different deNTXs doses (each group contained six mice)	61
Table 5 Necrosis scores under a fixed challenge dose (2MND) mixed with different dilution times of antivenom (AV)	62
Table 6 Comparison between the LD₅₀ and minimum necrotizing dose	63
Table 7 Taiwan Antivenom and Recommend doses.....	64

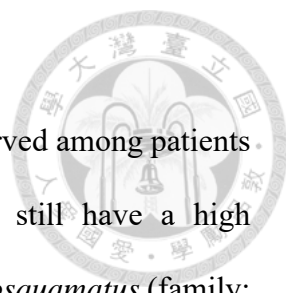
Chapter 1 Introduction

1-1 Snake classification and regional distribution in Taiwan

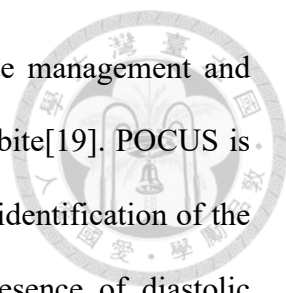
Taiwan is in a subtropical area that is indigenous to approximately 50 species of land snakes and six principal species of venomous snakes. The six major species of venomous snakes are *Bungarus multicinctus* and *Naja atra* in the Elapidae family; *Protobothrops mucrosquamatus*, *Trimeresurus stejnegeri stejnegeri*, and *Deinagkistrodon acutus* in the Crotalinae subfamily (family: Viperidae) and *Daboia siamensis* in the Viperinae subfamily (family: Viperidae) [1] (**Figure 1** and **Table 1**). Between 1904 and 1938, *T. s. stejnegeri* (47.3%) was the most commonly encountered snake throughout the island of Taiwan, followed by *P. mucrosquamatus* (26.0%), *B. multicinctus* (7.1%), *N. atra* (4.7%), *D. acutus* (1.9%) and *D. r. siamensis* (0.3%)[2]. Between 1986 and 1989, the 444 snakebite cases registered by the Taiwan National Poison Control Center (PCC) showed relatively equal incidences of encounters with *T. s. stejnegeri* and *P. mucrosquamatus* (22.3% vs. 22.1%)[3]. *P. mucrosquamatus* and *T. s. stejnegeri* snakebites are the most frequently reported snakebites in Taiwan[1]. *P. mucrosquamatus* is distributed on the whole island, and *Naja atra* is common in the central part of Taiwan; *D. acutus* is common in Hsinchu mountains, and *D. r. siamensis* is common in southern and eastern Taiwan [1,4]. In summary, in western Taiwan, *P. mucrosquamatus*, *T. s. stejnegeri* (subfamily: Viperidae) and *N. atra* (family: Elapidae) are the most encountered species responsible for snakebite.



1-2 Clinical presentation of snakebite



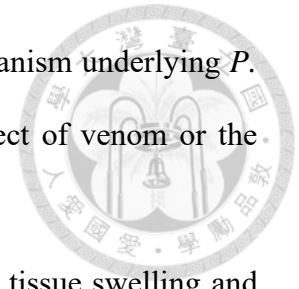
In Taiwan, a significantly improved survival rate has been observed among patients with snakebite who receive antivenom; however, these patients still have a high likelihood of developing local injuries [5]. Patients bitten by *P. mucrosquamatus* (family: Viperidae; subfamily: Crotalinae) present with tissue swelling and pain (96.2%) (**Figure 2**), local ecchymosis (57.5%), suspected wound infection (27.4%), bullae or blisters (23.1%) and wound necrosis (15.1%) (**Figure 3**) [6]. Severe tissue edema and severe pain in the bitten limb are the major concerns of Crotalinae snakebite-related injury. The symptoms mimic acute compartment syndrome (ACS), which is traditionally diagnosed based on the typical signs and symptoms, including the five Ps, i.e., pain, pallor, pulselessness, paresthesia and paralysis[7], and is usually seen as a surgical emergency [8,9]. The reported incidence of surgical intervention following snakebite injuries varies among hospitals in Taiwan, ranging from 6.6% to 24.3% for all types of snakebites and 0.7% to 49.7% for Crotalinae snakebites[2,4,10-12]. Because the clinical manifestations of snakebite envenomation may be confused with the clinical presentation of ACS, patients with snakebites often undergo decompression surgery, fasciotomy or fasciectomy, particularly if serial intracompartmental pressure (IP) measurements were not performed [13,14]. An objective evaluation of IP measurements has been recommended for patients with suspected snakebite-induced ACS, rather than evaluation only based on clinical symptoms [13,14]. A handheld manometer, such as the Stryker (Stryker Surgical, Kalamazoo, Michigan) [15] or C2DX device (The STIC Intra-Compartmental Pressure Monitor System, 555 East Eliza Street | Ste. A Schoolcraft, MI 49087) [16] or even a continuous pressure monitoring device (Mikro-Cath™ Pressure Catheter, Texas, USA)[17], is used to measure the IP [18]. However, this equipment might not be readily available in all emergency service settings. Since 2017, we have



applied point-of-care ultrasound (POCUS) (**Figure 4**) for snakebite management and decreased the rate of fasciotomy/fasciostomy in patients with snakebite[19]. POCUS is used to monitor the progression of local envenomation, namely, the identification of the location of edema (SCE or edema below the fascia) and the presence of diastolic retrograde arterial flow (DRAF) in the compressed artery [19]. Increased DRAF is observed in the affected artery in the same compartment where a restriction of the compartment space occurs, e.g., increased IP[20]. The noninvasive nature of POCUS theoretically minimizes bleeding complications following invasive catheter insertion in patients with coagulopathy following Viperidae envenomation [21]. POCUS provides an ideal tool for the serial evaluation of the location of edema and the presence of DRAF in the affected limb. POCUS is useful for facilitating clinical decisions for the treatment of snakebite envenomation-related acute compartment-like syndrome.

In addition to acute compartment-like syndrome, if the patient is bitten by *P. mucrosquamatus* over the finger or had blister formation, a high probability of necrosis formation is observed [6]. A 62-year-old male (**Figure 3**) was bitten by *P. mucrosquamatus* over the right thumb. He stayed in the emergency department (ED) for 50 hours and received 22 vials of antivenom. Fang marks, cyanosis, and ecchymosis were observed over the right thumb on arrival, and bullae formation was noted after 15 hours. Two weeks after this incident, he suffered from dry necrosis over the distal pulp of the thumb. According to the study by Dr. Mao (186 patients), the significant risks of *P. mucrosquamatus* snakebite-related wound necrosis include fingers as the bite site, blister formation and wound infection [6]. The anatomic site of the snakebite is an important factor affecting the prognosis of the wounds, i.e., digits are more likely to develop necrosis. The necrotic mechanism may involve the direct effect of the toxin, thrombotic microangiopathy [22-24] or increased pressure within the pulp space causing

compression of the digital arteries, resulting in ischemia. The mechanism underlying *P. mucrosquamatus* snakebite-related necrosis includes the direct effect of venom or the anatomical effect of the bite site, which requires further study.



Among patients bitten by *N. atra*, the symptoms include local tissue swelling and pain (94.5%), wound infection (80.9%), skin necrosis (65.6%), necrotizing soft tissue infection (42.1%), fever (32.3%), gastrointestinal effects (29%) and transient or partial ptosis or body weakness (4.9%) [5]. A 51-year-old male (**Figure 5**) who was bitten by *N. atra*, which was identified by the patient, received one vial of bivalent antivenom against *B. multicinctus* and *N. atra* and developed progressive necrosis two days later without any neurological symptoms. He underwent debridement several times and remained in the hospital for twenty-two days. The wound cultures showed infection with *Morganella morganii* and *Enterococcus faecalis*, which are commonly identified in patients who have been bitten by *N. atra* [25]. Patients bitten by *N. atra* develop delayed necrotic wounds, and an appropriate animal model is necessary to reproduce the venom cytolytic effects as in human.

Compared with the patient bitten by Crotalinae (*P. mucrosquamatus* and *T. s. stejnegeri*), the dermonecrosis presentation is common in the patients bitten by *N. atra*. The symptom that local injuries are more common than neurological toxicity after bites by many *Naja* species, including *N. nigricollis*, *N. mossambica*, *N. nigricincta*, *N. pallida*, *N. nubiae*, and *N. katiensis*, is also noted [26-28]. The mechanism was examined in many other species[28,29], but not *N. atra*.

1-3 Pathogenesis of snakebite-related dermonecrosis

Many animal studies have been designed to observe histological changes after snakebites.

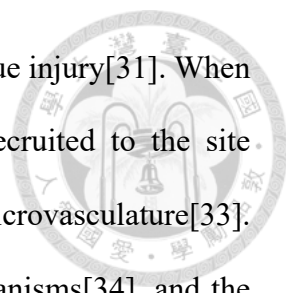


1-3-1 Progression of dermonecrosis

Mice were intradermally injected with the venom of spitting cobra (*N. nigricollis*). Five minutes later, signs of myonecrosis were present, including degeneration of the muscle layer, edema and vascular congestion[30]. One hour later, neutrophils infiltrated, and large amounts of neutrophils, eosinophils and macrophages and even fibrin deposition were observed in the blood vessels 24 hours later [30]. New epithelium and muscle layer formation were visible after 18 days, and granular scar tissue replaced the local tissue after 28 days [30]. In another mouse model intradermally injected with the venom of *N. nigricollis*, intradermal edema occurred between 30 mins and one hour, and blister formation occurred with a reduction in cellularity of the dermis three hours later [28]. Dermal necrosis, infiltration of many inflammatory cells and extensive thrombosis were noted at 24 hours [28]. Reepithelization and widespread collagen deposition in the dermis occurred by 14 to 28 days [28]. In summary, polymorphonuclear neutrophils are the first inflammatory cells to arrive and lead to the accumulation of infiltrating inflammatory cells, which was observed 3-6 hours after the injection and reached the highest level after 24 hours[31]. The effect of neutrophil-related immune reactions is associated with the development of myonecrosis and other types of tissue damage[28,32].

1-3-2 Neutrophil reaction

Neutrophils, which comprise 50-70% of circulating leukocytes in humans, have segmented nuclei and a cytoplasm enriched with granules and secretory vesicles [33]. Neutrophils are the first line of defense against microorganisms and play a role in



modulating inflammatory reactions in response to many types of tissue injury[31]. When tissue injury occurs or microorganisms invade, neutrophils are recruited to the site through rolling, adhesion, crawling, and transmigration from the microvasculature[33]. The main role of neutrophils is to isolate, engulf and kill microorganisms[34], and the defense mechanisms include phagocytosis, degranulation and release of neutrophil extracellular traps (NETs) [33,34]. Neutrophils endocytose opsonized bacteria into membrane-bound compartments, known as phagosomes, through macrophage receptor 1 (MAC1) and Fc receptors for IgG (FcγR)[34]. Phagosomes are then fused with several enzymes or granules (NADPH oxidase, elastase, gelatinase, BPI, azurocidin, lactoferrin, cathepsin G, defensins, myeloperoxidase and hydrochlorous acid) to become phagolysosomes and destroy bacteria [34]. Three types of granules have been identified in neutrophils: primary granules [myeloperoxidase (MPO), cathepsins, azurocidin, neutrophil elastase (NE), proteinase and defensins], secondary granules (collagenase, heparinase, gelatinase, lysozyme and sialidase) and tertiary granules (gelatinase and lysozyme)[34]. Degradation not only destroys microorganisms but also recruits additional neutrophils to the site, leading to tissue damage[35]. NETs are composed of web-like chromatin structures of DNA decorated with cytosolic and granule proteins for the purpose of binding and trapping microorganisms (including bacteria, fungi, viruses, and parasites) to neutralize, kill and prevent their dissemination [36,37]. The decorated proteins include histones, NE, MPO, calprotectin, cathelicidins, defensins and actins[38]. Two mechanisms of NET formation in response to different stimuli have been described. The first is a cell death pathway, also called NETosis, which is triggered by the generation of reactive oxygen species (ROS) by NADPH oxidase and begins with neutrophil depolarization, chromatin decondensation, nuclear delobulation and envelope formation and continues with granule membrane disintegration after stimulation for 3-8 hours

[38,39]. ROS activate MPO via the MEK (MAPK/ERK kinase)–extracellular signal-regulated kinase (ERK) signaling pathway and release NE, which degrades the actin cytoskeleton and is then translocated to the nucleus to drive chromatin decondensation[37]. Meanwhile, MPO also binds to chromatin and promotes decondensation by activating protein-arginine deiminase type 4 (PAD4), which citrullinates histones[37]. The second is a nonlytic NET that results in the rapid release of NETs through degranulation within minutes and occurs independently of cell death, but the mechanism is currently unclear[40,41]. Several human diseases are associated with NET formation[42], including snakebite-related injury[23,43]. After snakebite, the venom trapped by NETs and the granules decorated on NETs play roles in tissue damage[23]. In addition to the toxic effects of trapped venom and decorated granules, the formation of NETs may also promote microthrombosis formation, resulting in an ischemic microenvironment and worsening tissue damage[22]. In summary, snakebite-induced NETs may be a contributor to dermonecrosis, and the mechanisms include increased local levels of venom and granules and an ischemic microenvironment.

1-4 Features of venom

Snakebite-related local toxicity is usually presumed to be due to the action of phospholipase A₂ (PLA₂), cytotoxins (CTXs, also called cardiotoxins) and snake venom metalloproteinases (SVMPs) [21,44,45]. The components of the venom differ substantially between Viperidae and Elapidae. The components of *P. mucrosquamatus* (family: Viperidae; subfamily: Crotalinae) include SVMP (29.4%), C-type lectin (CLEC, 21.1%), snake venom serine protease (SVSP; 17.6%) and PLA₂ (15.9%)[46]. The average ratio of components in the crude venom of *N. atra* (family: Elapidae) is as follows: CTXs (56.2%), neurotoxins (NTXs, 22%); PLA₂ (15.4%) and high-molecular-weight proteins (HMWPs, 6.5%) [44,47]. The HMWPs include atrase B [48], atragin [49], kaouthiagin-like [49], and L-amino acid oxidase (LAAO) [50].

1-4-1 SVMPs, snake venom metalloproteinases

Four classifications of SVMP have been described. Class P-III SVMPs (63-66 kDa)[51] have been detected in all advanced snake families, including Elapidae and other evolutionary classes; P-II, P-I and P-IV are only detected in Viperidae[52]. P-I SVMP hydrolyzes the protein at the epidermal-dermal junction and leads to blister formation[52]. SVMP also results in myonecrosis in experimental models, but the mechanism is unknown and is possibly secondary to ischemia, which is the consequence of microvascular damage and defects in blood perfusion[52]. SVMPs destroy the capillary wall to alter the blood supply and then impair muscle regeneration, which is activated by myogenic stellate cells [52]. SVMP inhibitors have been administered to prevent Viperidae snakebite-related prominent local tissue injury[52]. SVMPs hydrolyze type IV collagen of the basement membrane of capillaries and release inflammatory mediators, inducing complement activation that is associated with the recruitment of

leukocytes and subsequent dermonecrosis[53,54]. SVMPs increase capillary permeability and induce edema [53]. SVMPs also activate endogenous matrix metalloproteinases (MMPs), which may contribute to extracellular matrix (ECM) degradation [55]. The combined effects of SVMPs and MMPs results in local tissue damage during envenomation following a Viperidae snakebite.

1-4-2 PLA₂, phospholipase A₂

PLA₂ is a unique calcium-dependent hydrolytic enzyme that hydrolyzes glycerophospholipids to lysophospholipids and free fatty acids[56], and includes sPLA₂ (secretory PLA₂), iPLA₂ (Ca²⁺-independent PLA₂), cPLA₂ (cytosolic PLA₂), and PAF-AH (platelet-activating factor acetylhydrolases); they are classified into fourteen groups [57]. Snake venom contains sPLA₂ that is categorized into Groups I and II, which are low molecular weight proteins (13-14 kDa) [58]. The PLA₂ of the Elapidae is a Group I PLA₂ and that of the Viperidae is a Group II PLA₂ [57]. PLA₂ activity depends on the binding of Ca²⁺ and the substrate, formation and catalysis of intermediates, and release of the reaction products[59]. PLA₂ induces local tissue edema by hydrolysis and phospholipid production and then releases arachidonic acid. Arachidonic acid is converted to prostaglandins and leukotrienes, which induce increased vascular permeability and local edema[60,61]. PLA₂ enzymatically hydrolyzes phospholipids and has a nonenzymatic function as an agonist or antagonist of the target proteins[57]. The pharmacological effects of PLA₂ mainly depend on the high affinity of the protein–protein interaction between PLA₂ and membrane proteins in the specific target tissue[62]. Therefore, PLA₂ exhibits a wide variety of pharmacological effects, including presynaptic or postsynaptic neurotoxicity[63], hemolytic activity[64], cardiotoxicity[65] and myotoxicity[66]. Unlike SVMPs, PLA₂ promotes diffuse myonecrosis but does not affect the microvascular circulation[52]. PLA₂ hydrolyzes phospholipids to form lysophospholipids and free fatty

acids[57] and therefore disrupts the integrity of the plasma membrane of muscle fibers[46,67] and induces a signaling cascade, including calcium influx and mitochondrial dysfunction, resulting in muscle cell damage [68,69]. PLA₂ and LAAO are proposed to induce oxidative stress and lead to cell death[69].

1-4-3 CTXs, cytotoxins (also called cardiotoxins)

CTXs are small nonenzymatic proteins (6-7 kDa)[70] that are members of the three-finger toxin (3FTX) family, which shares a common structure of a three beta stranded loop extending to a central core cross-linked by four conserved disulfide bridges [71-73]. CTXs are abundant in the Elapidae family, particularly in cobra [74-76]. CTXs constitute approximately 50% of the dry weight of crude cobra venom and are highly lethal; they also exert various pharmacological effects[71,76]. Different mechanisms of CTX-related cytolytic effects have been discussed. Some studies have revealed that CTXs interact with lipid membranes and then lead to membrane damage and necrotic cell death [70,77]. Some studies have shown that CTXs penetrate cells and trigger cytolytic activity[67]. Additionally, CTXs activate mitochondria to induce the cell death pathway and subsequent programmed cell death pathway[78]. Many subtypes of CTXs have been identified, including types I, II, III, and IV, and all have cytolytic activity [45]. PLA₂ and CTXs are suspected to be the major causes of the local injuries induced by *N. atra* bites[45].

1-5 Evaluation of the venom-induced cytotoxic effect

Traditionally, antivenom is evaluated based on the 50% effective dose (ED_{50}), which is based on the 50% lethal dose (LD_{50}) of crude venom in mice [79,80]. The effectiveness of traditional antivenom does not consider cytolytic effects and is evaluated based on the improvement in the survival rate. Therefore, the World Health Organization (WHO) suggested using the minimum necrotizing dose (MND) of venom as a method for evaluating the neutralizing effect of antivenom [81]. The MND of venom is the smallest dose that leads to the development of a necrotic lesion 5 mm in diameter after an intradermal injection into the dorsal skin of mice [81]. The MND_{50} is the value used to evaluate the neutralizing effect of antivenom on venom-induced necrosis [81].

1-6 AIM

In clinical practice, antivenom indeed improves snakebite-induced systemic toxicity; however, it seems to exert limited effects on local injuries, including progressive swelling and dermonecrosis. Intervention with the POCUS protocol may facilitate clinical decisions for treating snakebite envenomation, especially acute compartment-like syndrome. Snakebite-envenomated patients who develop dermonecrosis are usually observed after a *Naja atra* bite in Taiwan and the symptoms occur in the next 48 to 72 hours. Indirect tissue injury caused by immune reactions, such as neutrophil extracellular traps (NETs) triggered by snakebite envenomation and the direct effect of different components of venom, are possible mechanisms of dermonecrosis. Further studies are still needed to assess *N. atra*-related dermonecrosis. In previous studies using animal models, mice injected with the crude venom of *N. atra* did not survive long enough to develop the necrotic wounds observed in humans [82]. The AIM of this study is to evaluate the mechanism of *N. atra* snakebite-related dermonecrosis via the formation of NETs and to clarify the major component of venom.

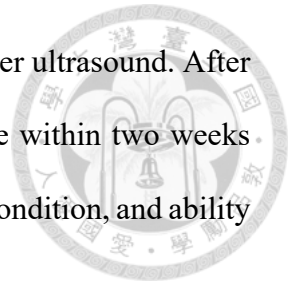
Chapter 2 Materials and Methods



2-1 Patient recruitment

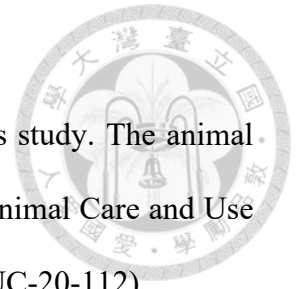
Tri-Service General Hospital is a medical center located in northern Taiwan in the Neihu area and is surrounded by mountains. Tri-Service General Hospital receives patients with snakebite from the Jinshan, Wanli, and Ruifang Districts, as well as from Keelung City. Approval was obtained from the Institutional Review Board of the Tri-Service General Hospital (1-106-05-103). The species of snake involved, the time of year of the bite, the site of the bite, the sex and age of the patients and the outcomes of patients (hospitalization days, surgical intervention, and ED stasis time) were reviewed manually. We reviewed the medical records before 2009-2016 and recruited new patients since 2017. This study employed a prospective design. Approval was obtained from the Institutional Review Board of the Tri-Service General Hospital (TSGH IRB No.: 2-107-05-039). Each patient provided written informed consent prior to enrollment. All patients with snakebite arriving at the hospital within the study period were managed by doctors experienced and trained in snakebite treatment. The patients' general data, event location, wound type and activity were recorded. The snake that bit each patient was categorized as "identified", "suspected" or "unidentified". The snakes were identified when the patient brought the snake or took pictures of the actual snake that bit him or her, and this identification was confirmed based on illustrations of the snake by experts specializing in snakebites. The choices of antivenom were bivalent antivenom for *B. multicinctus* and *N. atra* or for *P. mucrosquamatus* and *T. stejnegeri*, which were manufactured by the National Health Research Institutes, Miaoli, and distributed by the Centers for Disease Control, Taiwan [83]. All patients followed the management protocol summarized in the flow chart[3]. All patients were also examined using POCUS to define the extent of the

edema and to scan the target artery proximal to the lesion with Doppler ultrasound. After discharge from the hospital, all patients were followed by telephone within two weeks and at the outpatient clinic. Complications, repeated surgery, wound condition, and ability to perform daily activities were recorded.

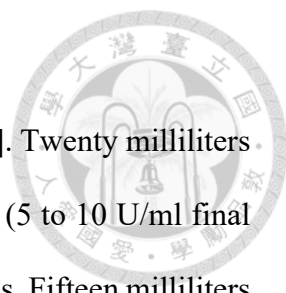


2-2 Animals

Male CD-1 mice (10-12 weeks old, 20-22 g) were used in this study. The animal handling protocol was reviewed and approved by the Institutional Animal Care and Use Committee (IACUC) of the National Defense Medical Center (IACUC-20-112).

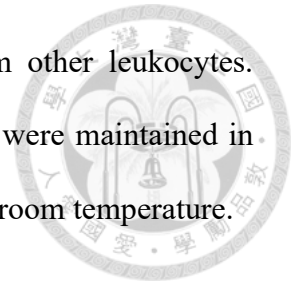


2-3 Human neutrophil isolation



The isolation method was modified from other studies[40,84,85]. Twenty milliliters of blood were collected from healthy adult males in sodium heparin (5 to 10 U/ml final concentration) or acid citrate dextrose (ACD-A) blood collection tubes. Fifteen milliliters of HBSS (–) were dispensed into a 50-ml conical centrifuge tube and blood was transferred to the tube. The blood mixture was underlaid with 12 ml of Ficoll-Paque Premium (Cytiva 17-5442-02, pack of 6 × 100 mL, cat. No. GE17-5442-02). The tube was centrifuged at 500 G for 30 min at room temperature, with the brake off. Mononuclear cells, remaining plasma, and Ficoll-Paque Premium were aspirated from the tube, leaving the PMN- and erythrocyte-rich pellet. The pellet was diluted with HBSS (–) to a final volume of 20 ml. Twenty milliliters of 3% dextran were added and the tube was inverted several times to mix. Erythrocytes were sedimented under gravity for 20 min at room temperature. The PMN-rich supernatant was transferred to a new tube and diluted with HBSS (–). The sample was centrifuged at 300 G for 10 min at room temperature. The supernatant was aspirated, and the remaining erythrocytes were lysed with 10 ml of hypotonic lysis buffer and incubated for no more than 30 sec, followed by the quick addition of 10 ml of re-equilibration buffer to restore isotonicity. The sample was diluted further with 30 ml of HBSS (–). The mixture was centrifuged at 300 × g for 10 min at room temperature, the supernatant was aspirated, and the preceding step was repeated once before the cells were washed with 30 ml of HBSS (–). The lysis procedures was repeated if significant erythrocyte contamination was observed. Cells were resuspended in 1 to 2 ml of HBSS (–). Cells were counted using an automated cell counter. Alternatively, 10 µl of cells were diluted in 490 µl of 3% acetic acid and counted with a hemocytometer (APPENDIX 3A; Strober, 1997). Notably, 1 to 2 × 10⁶ PMNs were isolated per ml of whole blood with >95% purity and viability. Acetic acid enhances the

nuclear morphology, permitting the differentiation of PMNs from other leukocytes. PMNs must be studied immediately after isolation. Purified PMNs were maintained in HBSS (–) at concentrations ranging from 1 and 2.5×10^7 cells/ml at room temperature.



2-4 Western blot analysis of snake venom-induced NET formation

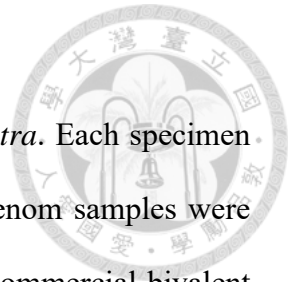
The western blot analysis was modified from the study by Wong, S. L., et al.[86]. Isolated neutrophils were mixed with 100 nM PMA (phorbol 12-myristate 13-acetate (PMA), PKC activator, Cat. No. ab120297) as a positive control. The isolated neutrophils were mixed with different concentrations (5 µg/ml, 25 µg/ml, or 50 µg/ml) of lyophilized crude venom dissolved in HBSS(-) and incubated for 180 minutes. Levels of H3Cit and PAD₄ in human neutrophils were quantified using western blotting. Isolated human neutrophils were homogenized in RIPA buffer supplemented with a protease inhibitor cocktail (Sigma) on ice. The sample was centrifuged at 20,000 g for 20 min at 4 °C. The protein content in the supernatant was determined using bicinchoninic acid protein assay and an equal amount of protein from each sample was resolved on gradient gels (5, 10, and 12% Tris-Glycine gels, Life Technologies) and electroblotted (80 V for 30 minutes and then 90 V for 140 minutes) onto PVDF membranes, which were then incubated with primary antibodies (mouse monoclonal anti-PADI4/PAD4 antibody [OTI4H5], 1:1000, cat.no. no. ab128086; rabbit polyclonal anti-histone H3 antibody-nuclear loading control and ChIP grade, 1:1000, cat. no. ab1791; rabbit polyclonal anti-histone H3 (citrulline R2 + R8 + R17) antibody-ChIP grade, 1:1000, cat. no. ab5103; and mouse monoclonal anti-GAPDH antibody [6C5], 1:1000, cat. ab8245) at 4 °C overnight and subsequently with appropriate HRP-conjugated secondary antibodies (1:5,000 dilution of HRP-conjugated goat anti-rabbit IgG (H+L), Bio-Rad, cat. no. 170-6515; 1:10,000 dilution of HRP-conjugated goat anti-mouse IgG (H+L), Bio-Rad, cat. no. 170-6516; or 1:5,000 dilution of HRP-conjugated goat anti-rat IgG (H+L), Invitrogen, cat. no. A10549) for 2 h at room temperature. The blots were developed with enhanced chemiluminescence substrate (Thermo Scientific, cat. no. 32106). Equal loading was confirmed by probing for GAPDH (1:40,000, Ambion, cat. no. AM4300). Blots were quantified using ImageJ software.

2-5 Chemicals and reagents

Phorbol 12-myristate 13-acetate (PMA), a molecule that activates protein kinase C (PKC) and triggers reactive oxygen species (ROS) production, was used as a positive control for NET formation [37]. Trifluoroacetic acid (TFA), ammonium bicarbonate (ABC), formic acid (FA), dithiothreitol (DTT), iodoacetamide (IAM), and Tween 20 were purchased from Sigma–Aldrich (MO, USA). Sodium hydroxide, DMSO, iodomethane and trichloromethane were purchased from Merck Millipore (Darmstadt, Germany). Trypsin was purchased from Promega (15,664 units/mg, sequencing grade, WI, USA). Acrylamide, SDS and TEMED were obtained from Bio-Rad (USA). Acetonitrile (ACN) was purchased from J.T. Baker (Phillipsburg, NJ, USA). Deionized water was generated with a Simplicity Ultrapure Water System (Millipore, USA) and had a measured value of 18 MΩ.

2-6 Snake Venom Approach and Analysis

Venom was collected from 10 healthy adult specimens of *N. atra*. Each specimen was manually restrained, and the venom was milked. The liquid venom samples were individually obtained, lyophilized, and stored at -80 °C until use. Commercial bivalent equine antivenom intended for clinical usage and antivenin against the venom of *B. multicinctus* and *N. atra* (trade name: Antivenin of *B. multicinctus* and *N. atra* (lyophilized); 1000 antivenom units/vial; bench number: 61-06-0010) were produced at the Taiwan Centers for Disease Control (CDC).



2-7 Preparation of deNTXs, deNTXs-deCTXs, and deNTXs-dePLA₂

Lyophilized crude *N. atra* venom was dissolved in water and centrifuged at 10,000 g for 10 min. The amount of protein in the venom was determined using a BCA Protein Assay kit (PierceTM, Thermo Scientific). The supernatants were diluted and further purified using size exclusion chromatography. The purified venom proteins, NTXs, were isolated from crude venom using the procedure described by Huang et al. [47]. All venom protein components other than the NTXs were combined and dissolved in PBS, creating deNTXs. The crude venom and deNTXs were loaded onto a Phenomenex Jupiter® C18 (250 x 4.6 mm, 5 µm particle size, 300 Å pore size) column and separated with an ultraperformance liquid chromatography (UPLC) system (LC-20ADXR, Shimadzu, Kyoto, Japan) equipped with a DAD detector (SPD-M20A, Shimadzu, Kyoto, Japan) and autosampler (SIL-20ACXR, Shimadzu, Kyoto, Japan). The venom components were eluted at a rate of 1 mL/min with a linear gradient of 0.1% TFA in water (Solvent A) and 0.1% TFA in 100% ACN (Solvent B) (2% B for 5 min, followed by 2-10% B for 2 min, 10-16% B for 6 min, 16-28% B for 2 min and 28-65% B for 37 min) [47]. Protein elution was monitored at 215 nm (absorption wavelength for peptide bonds). The relative abundance (expressed as the percentage of the total venom protein) of each protein family was estimated using the method described by Huang et al. [47].

2-8 Minimum Necrotizing Dose (MND)

According to the WHO Expert Committee on Biological Standardization [81], the MND of venom is the smallest amount of venom (in μg of dry weight) that leads to the development of necrotic lesions 5 mm in diameter 3 days after intradermal injection into the dorsal skin of lightly anesthetized mice. CD1 mice (10–12 weeks old) were obtained from BioLASCO Taiwan Co. Ltd. (Taipei, Taiwan) and randomly divided into groups (6 mice/group). The fangs of *N. atra* are noticeably short [1,29]. We used intradermal injections to simulate real-world conditions. The fur was removed from the dorsal skin of one group of mice and 50 μL of sterile saline was intradermally injected; these mice served as the control group. Next, the mice in the testing groups underwent removal of the fur from the dorsal skin and received a single intradermal injection of deNTXs (16.5, 20.5, 25.5, 32, and 40 μg). The diameter of the necrotic area of the dorsal skin was measured after 72 hours. The MND was determined with linear interpolation.

2-9 MND50: Efficacy of Antivenom Neutralization

The MND₅₀ is a measure of the ability of an antivenom to prevent venom-induced dermonecrosis [81]. The MND₅₀ is identified as the dose of antivenom (in microliters) that results in a diameter of the necrotic lesion that is 50% smaller than that of the lesion induced by the injection of venom and saline [81]. Two times the MND of deNTXs was selected as the challenge dose. The antivenom was bivalent against *B. multicinctus* and *N. atra*, which was manufactured by the National Health Research Institutes, Miaoli, and distributed by the Taiwanese Centers for Disease Control, Taiwan. [3]. A fixed dose of venom was incubated with various dilutions of antivenom for 30 min at 37 °C. The positive control was venom incubated with saline instead of antivenom. Then, aliquots of 0.5 mL of the mixtures containing an amount of venom corresponding to 2 times the MND were injected intradermally into groups of six CD1 mice (10–12 weeks old).

2-10 Biopsy and Necrosis Score

The mice were intradermally injected with deNTXs (0.5, 0.33, 0.22, 0.148, and 0.098 $\mu\text{g/g}$) or 2 times the MND with different dilutions of antivenom (from the original concentration: 1:2, 1:3, 1:4 and 1:5) into the dorsal skin. After 72 hours, the mice were euthanized, and the dorsal skin was removed and sent for skin biopsy and hematoxylin and eosin (HE) staining. Then, the biopsy was scored (**Table 3**) by an animal pathologist based on necrosis.

2-11 Point-of-care ultrasound (POCUS)

We used two sonography machines, Sparq and CX50 (Philips ultrasound, Inc. software version: 4.0.2; 22100 Bothell Everett Highway, Bothell, WA 98041 U.S.A.), which were equipped with 15-MHz linear probes. POCUS was performed by experienced emergency physicians on duty. We used two methods to evaluate the patients. The first method determined the location of edema. We used the soft-tissue mode and obtained images in the transverse and longitudinal planes of 3-5 sites surrounding the area of the snakebite starting from the site of maximal swelling and progressing proximally until normal soft tissue was noted. Using the first method, we evaluated edema based on the characteristic cobblestone-like appearance [87]. The cobblestone-like appearance indicates a hyperechoic, hyperemic pattern of subcutaneous fat surrounded by anechoic fluid, which indicates inflammatory tissue and the extravasation of fluid due to increased permeability [87,88]. We used the relative locations of the cobblestone-like tissue and the fascia to evaluate whether the edema was located in the fascia or the subcutaneous area. We assessed the separation of the cobblestone-like tissue and normal tissue each hour until the swelling improved and marked the area to determine the rate of proximal swelling [89]. The second method was performed to determine the pulsed Doppler signal of the target artery proximal to the compressed area. DRAF was considered present when the artery was compressed[20]. A 15-MHz linear probe was used with the vascular mode, and Doppler velocity tracings were obtained in the transverse view and transferred to the longitudinal direction. The dorsalis pedis artery, popliteal artery, radial artery and brachial artery were evaluated in patients who had been bitten on the foot, lower leg, hand and forearm, respectively, to simulate the setting used in the study by McLoughlin et al.[20], in which the artery proximal to the compressed area was detected. Since the most common bite sites were the hands and feet, the dorsalis pedis artery and radial artery were usually

the target arteries in the current study[19]. Pulse wave tracing was performed with an insonation angle of less than 60 degrees over the target artery to identify the systolic and diastolic waves [20]. Baseline Doppler measurements of the artery were also obtained at an unaffected site to account for age-dependent arterial wall impairments [90,91].

2-12 data analysis

We report the data as the means \pm standard deviations (SDs). Statistical analyses were performed using t test, one-way ANOVA and Bonferroni's multiple comparisons test with Prism 6 software (GraphPad Software, Inc., USA). Kruskal-Wallis test was used to analyze the variation of tissue score evaluation under different level of venom and mixture of antivenom. Statistical differences were considered significant when p was \leq 0.05.

Chapter 3 Results



3-1 Crude *N. atra* venom induces NET formation

Neutrophils were isolated from healthy adults and mixed with phorbol 12-myristate 13-acetate (PMA) for 4 hours to induce NET formation, which were stained with Wright and Giemsa stain as the positive control (**Figure 6**). Different concentrations (5 $\mu\text{g/ml}$, 25 $\mu\text{g/ml}$, and 50 $\mu\text{g/ml}$) of crude *N. atra* venom were mixed with neutrophils, incubated for 180 min, and the levels of PAD4, H₃, H₃Cit, and GAPDH were quantified using western blot analysis (**Figure 7**). The formation of PAD4 or H₃Cit indicates NET formation[92]. The activation of PAD4 citrullinates histone H₃ to produce H₃Cit [37]. These results indicate that the crude *N. atra* venom induced NET formation. The level of NETs seems to correlate with the venom concentration. Decreased levels of PAD4 and H₃Cit were noted in cells treated with the highest concentration (50 $\mu\text{g/ml}$) of crude venom.

3-2 Characterization of *Naja atra* Crude Venom and the MND of the deNTXs

The crude *N. atra* venom contained NTXs, PLA₂, CTXs, cysteine-rich secretory proteins (CRISPs) and high-molecular-weight proteins (HMWPs) (**Figure 8**). We removed the NTXs (the lethal component) from the crude venom, creating a venom devoid of NTXs (deNTXs) (**Figure 8**). All mice that were intradermally injected with the deNTXs survived for three days, and necrotic changes were observed, similar to human wounds (**Figure 9**). Different concentrations of deNTXs were tested, and the MND of the deNTXs in mice was 0.494 ± 0.029 $\mu\text{g/g}$ (injection volume: 50 μL , mouse weight: 20–22 g) (**Table 2**).

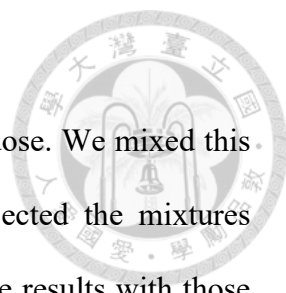
3-3 CTXs are the Major Component Causing Necrosis

Furthermore, we determined which component played the most important role in inducing necrosis by separately removing the CTXs and PLA₂ from the deNTXs. The MND of deNTX-dePLA₂ (major component retained: CTXs) was 0.294 ± 0.050 $\mu\text{g/g}$, and the MND of deNTX-deCTXs (major component retained: PLA₂) was greater than 1.25 $\mu\text{g/g}$ (**Figure 10** and **Table 2**). The results showed that CTXs played a major role in the mechanism generating necrosis.

3-4 Development of Necrosis

After determining the MND, we established a series of low concentrations of deNTXs to investigate the mechanism underlying the development of necrosis. Mice were injected intradermally with different concentrations (0.5, 0.33, 0.22, 0.148, and 0.098 $\mu\text{g/g}$), and necrotic changes were observed after 72 h (). We removed the necrotic skin and sent it for biopsy. Necrosis was scored by a veterinary pathologist. The severity of necrosis was classified as normal (score of 0), minimal (score of 1), mild (score of 2), moderate (score of 3), or severe (score of 4) (**Table 3**). In the biopsy, severe necrosis appeared as the loss of organization and a substantial increase in tissue space. Skin biopsies were evaluated in individual layers, namely, the epidermis, dermis, hypodermis, panniculus carnosus and adventitia. Even when the dose was less than the MND ($0.494 \pm 0.029 \mu\text{g/g}$), 0.098 $\mu\text{g/g}$ deNTXs still induced necrosis, and the pathology extended deeper than the dermis. The most severely destroyed layer was the panniculus carnosus and adventitia, even after treatment with the minimum dose (**Figure 11**, **Figure 12** and **Table 4**).

3-5 Neutralization Ability of the Antivenom

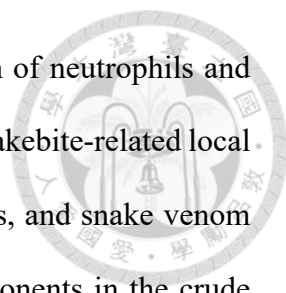


We used two times the MND of the deNTXs as the challenge dose. We mixed this dose with different dilutions of antivenoms in vitro and then injected the mixtures intradermally into each mouse (5 mice per group). We compared the results with those from mice injected with a challenge dose mixed with saline to identify the MND₅₀, according to the recommendation of the WHO [81]. The mice injected with the challenge dose mixed with saline developed necrotic lesions with diameters of approximately 7 mm. The other mice injected with different dilutions of antivenom (from the original concentration to a 1:5 dilution) still had necrotic lesion diameters that were greater than 5 mm. None of the mice developed necrotic lesion diameters that were 50% smaller than those in the mice injected with two times the MND mixed with saline. Therefore, we were unable to identify the MND₅₀ with this antivenom. The necrotic lesions were biopsied, and necrosis was scored in the individual skin layers (**Figure 13, Figure 14 and Table 5**). Regardless of the concentration of antivenom, including the original concentration, the challenge dose of the deNTXs resulted in necrosis throughout all the layers of the skin, including severe necrosis in the panniculus carnosus and adventitia.

Chapter 4 Discussion



G. D. Katkar et al. first reported the association between the formation of NETs and snake venom[23]. Venom from *Echis carinatus* (subfamily: Viperinae) induces the formation of NETs, which trap venom and lead to local necrosis [23]. Methods designed to destroy the NET structure or to compensate for neutropenia diminish the local necrotic effect and disseminate snake venom, which increases systemic toxicity and even the mortality rate in the animal [23]. *B. Swethakumar* et al. documented that crude venom of *E. carinatus* induced NETosis (suicidal type) and that *N. atra* venom induced nonlytic NETs (vital type) [93]. However, the occurrence and types of NETs are still debated, possibly due to the biodiversity of species, even venom from the same species of snake [23,31,94]. In our study, we showed that crude venom of *N. atra* induced NETs by performing a western blot analysis of PAD₄ and H₃Cit levels (**Figure 6**). The crude venom of *N. atra* activated PAD₄, which citrullinates histone H₃ to generate H₃Cit [37]. The formation of NETs correlated with the venom concentration and decreased when a high venom concentration (50 µg/ml) was administered, like other studies[93]. The granules decorating the chromosomes in NETs or the trapped venom may increase the local venom concentration and then exacerbate local damage. A higher concentration (50 µg/ml) of venom may result in cell death without NET release. The formation of lytic or nonlytic type of NETs in response to envenomation still requires further study. CTX-1 induces the death of leukemia cell lines U937 and HL-60 through Fas and ATF-2-mediated FasL transcription via the Ca²⁺/NOX4/ROS/p38 MAPK axis[95]. We suspect that ROS are produced through a mechanism mediated by the CTX-1-related FasL/Fas death pathway, which leads to NETosis (suicidal-type NETs) and even cell death in the presence of higher concentrations of CTX-1.

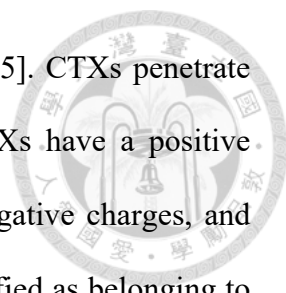


The early presentation of myonecrosis before the accumulation of neutrophils and macrophages may indicate a direct cytolytic effect of venom [30]. Snakebite-related local toxicity is usually presumed to be due to the actions of PLA₂, CTXs, and snake venom metalloproteinases (SVMPs) [21,44,45]. The average ratio of components in the crude venom of *N. atra* (family: Elapidae) is as follows: CTXs (56.2%), neurotoxins (NTXs, 22%); PLA₂ (15.4%) and high-molecular-weight proteins (HMWPs, 6.5%) [44,47]. Therefore, the targets potentially causing dermonecrosis in this study are CTXs and PLA₂. Dermonecrosis induced by envenomation from *N. nigricollis* has been discussed in several studies [28,30]. Crude venom was used in these studies; however, the crude venom of *N. atra* resulted in animal death before dermonecrosis occurred[82]. The 50% lethal dose (LD₅₀) of crude venom from *N. atra* is 0.56 µg/g[45,96,97] and the value of crude venom from *N. nigricollis* is 2 µg/g[98] Compare the level of NTX between *N. atra* and *N. Nigricollis*, the later had less level of NTX[47,99]. Unlike the study of *N. nigricollis*, the lethal component of the venom from *N. atra* must be knocked out to mimic human dermonecrosis in an animal model. The most lethal components of *N. atra* venom are NTXs[45]. NTXs are members of the three-finger toxin (3FTX) family[71] with a low molecular weight of approximately 7 kD[100]. NTX targets acetylcholine receptor (AchR), which influences the proliferation of lymphocytes[101], and functions as an antagonist of postsynaptic nicotinic receptor, which blocks the neuromuscular junction[44,102]. Neuromuscular blockade, which results in flaccid paralysis and respiratory failure, is the main mechanism by which NTX leads to death [44,102,103]. We suspected that the NTXs in *N. atra* venom might have a relatively low affinity for human neuroreceptors or another yet unknown mechanism explained why people bitten by *N. atra* develop few neurological symptoms [5]. In people who have been bitten by *N. atra*, the NTXs do not lead to immediate mortality, allowing the other toxins time to cause

necrosis. Patients bitten by *N. atra* developed delayed necrotic wounds, and deNTXs were necessary for mice to survive long enough to develop cytolytic effects.

The traditional method of evaluating the antivenom effect by calculating the LD₅₀ and 50% effective dose (ED₅₀) may not be suitable for the assessment of venom-related cytolytic effects. Traditionally, antivenom is evaluated based on the ED₅₀, which is based on the LD₅₀ of crude venom in mice [79,80]. Mice injected with the crude venom of *N. atra* do not survive long enough to develop the necrotic wounds observed in humans [82]. Methods to evaluate the progression of snakebite-related edema and a suitable animal model to assess the cytolytic effect of the venom are needed. The LD₅₀ of crude venom injected intravenously into adult mice was 0.56 µg/g[45,96,97]. NTXs are a lethal component of crude venom, and the LD₅₀ of intravenously injected NTXs was 0.075 µg/g [45]. After the NTXs were removed, the MND of the deNTXs was found to be 0.494 ± 0.029 µg/g (**Table 6**). An evaluation of the ability of antivenom to neutralize the LD₅₀ in mice alone is not adequate for assessing necrosis. The MND identifies the necrotic effect of the venom, and the MND₅₀ refers to the antinecrotic effect of the antivenom [81].

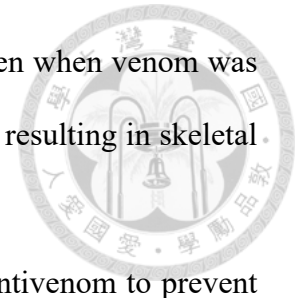
Both CTXs and PLA₂ are suspected to be the major components of the venom of *N. nigricollis* that cause dermonecrosis [28]. In the present study, we identified a major role for CTXs in the mechanism by which the venom of *N. atra* caused necrosis. CTXs are less toxic than NTXs, although they exert cytotoxic effects that contribute to the lethality of venom [45]. Many subtypes of CTXs have been identified, including types I, II, III, and IV, and all possess cytolytic activity [45]. CTX was the major cause of snake venom related dermonecrosis possible through the mechanisms of interact with lipid membrane and then lead to membrane damage and necrotic cell death [70,77] or direct penetrate cells[67], even activate mitochondria to induce the cell death pathway and subsequent programmed cell death pathway[78]. In the latest study, CTX may also activate the Ca²⁺



/NOX₄ /ROS/p38 MAPK axis then resulting in cytotoxic effects [95]. CTXs penetrate cell membranes by damaging the phospholipid bilayer [104]. CTXs have a positive charge and easily bind to membranes and vesicles, which have negative charges, and tighter binding leads to increased cellular lysis [103]. PLA₂ is classified as belonging to Group I (Elapidae) and Group II (Viperidae) [105]. In addition, PLA₂ is proposed to play a role in local muscle injury. In the present study, significant variation was noted when we compared the MND of deNTXs-dePLA₂ (major component retained: CTXs) with the MND of deNTXs-deCTXs (major component retained: PLA₂) (0.294 ± 0.050 µg/g vs. greater than 1.25 µg/g). We suspected that necrosis was mainly caused by CTXs, and no significant synergistic effects of CTXs and PLA₂ were observed. Similarly, the use of a PLA₂ inhibitor did not decrease the necrotic area caused by *N. nigricollis* venom [28]. PLA₂ is an isoenzyme, and one snake may produce more than one isoenzyme[57,106]. PLA₂ interacts with other proteins to form aggregates that contribute to the enzymatic activity of PLA₂[57,107]. This phenomenon is important for the pharmacological potency and toxicity of PLA₂ toxins, which may explain our results. However, we were unable to investigate whether NTXs exerted synergistic effects between each venom in this study.

The fangs of *N. atra* are noticeably short [1,29]. We used intradermal injections to simulate real-world conditions. As observed in the biopsy specimen, the venom was injected into the intradermal layer, after which the venom penetrated deeper rather than spreading along the surface. The deNTXs were distributed throughout the soft tissue rather than remaining localized at the site of injection, and severe damage was observed in the panniculus carnosus and adventitia, even at low concentrations that are also noted in the snakebite by *N. nigricollis* [30]. The venom may penetrate the layers and be transported into the circulation by the lymphatic system [108]. This observation would explain the development of myotoxicity after the progression of necrosis, even given the

short fang length [28]. As described in the study by Iddon et al., even when venom was injected intradermally, it penetrated deep into the layers of the skin, resulting in skeletal muscle injury[30].



Some animal studies have investigated the administration of antivenom to prevent venom-related dermonecrosis [28,30]. A significantly improved survival rate has been observed among patients with snakebite who receive antivenom [2,5]. In Taiwan, horse-derived antivenom is manufactured by the National Health Research Institutes, Miaoli, and distributed by the Centers for Disease Control, Republic of China, Taiwan[2,3]. Four types of antivenom are available in Taiwan, which are all F(ab²) fragments in lyophilized form [83,109]. The antivenoms are a bivalent antivenom against *P. mucrosquamatus* and *T. s. stejnegeri*, a bivalent antivenom against *N. atra* and *B. multicinctus*, a monovalent antivenom against *D. acutus*, and a monovalent antivenom against *D. r. siamensis* [83,110]. The National Poison Control Center of Taiwan (PCC-Taiwan) recommended antivenom doses (**Table 7**) of 1–2 vials for *T. s. stejnegeri*, 2–4 vials for *P. mucrosquamatus*, 2–4 vials for *D. acutus*, 2–4 vials for *D. r. siamensis*, 6–10 vials for *N. atra*, and 2–4 vials for *B. multicinctus*, which were based on the LD₅₀ for crude venom in mice[3]. These antivenoms are effective at alleviating systemic toxicity in humans, such as *B. multicinctus*-related respiratory failure[111], *D. acutus* and *D. r. siamensis*-related thrombocytopenia and coagulopathy[112]. According to many clinical observation studies, the median dosage of antivenoms is higher than the PCC-Taiwan recommendation, such as 5.5 vials for *P. mucrosquamatus*[6], 5 vials for *T. s. stejnegeri*[113], 10 vials for *N. atra*[5], and 4+4 vials for *B. multicinctus*[111]. Even when patients receive antivenom, wound dermonecrosis or progressive swelling still occurs[5]. In clinical practice, antivenom indeed improves snakebite-induced systemic toxicity; however, it seems to exert limited effects on local injuries, including progressive swelling

and dermonecrosis. Therefore, clinicians have increased the doses of antivenom when the local injury persists.

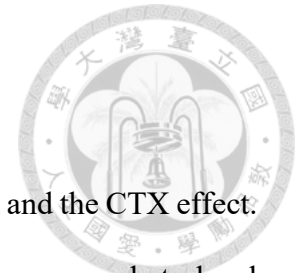
In Taiwan, the antivenom administered to patients who have been bitten by *N. atra* is a bivalent freeze-dried neurotoxic antivenom (FNAV) against *B. multicinctus* and *N. atra* [114]. The equine antivenom produced by the injection of crude venom from *N. atra* may not induce the production of adequate antibodies against CTXs. In this study, we determined the MND of the deNTXs, and the MND₅₀ was unable to be determined, suggesting that the antivenom did not effectively neutralize the CTXs. In the study by Wu et al., the neutralization efficacy of antivenom was poor for CTXs A2, 4 and 5 [47]. As mentioned above, CTXs play a major role in necrosis. The polyvalent antivenom generated in horses after a challenge with crude venom does not neutralize the CTXs, which might explain why it is ineffective at preventing necrosis. Other antivenoms also have little to no effect on local damage [82,115]. In addition to the poor neutralization ability, the early direct effect of venom on inducing cytolytic injury may be another explanation for the inefficiency of antivenom [30]. Administration of antivenom as soon as possible is recommended to effectively neutralize the cytolytic effect of the venom and is significantly dependent on the duration between venom injection and administration of antivenom [30,116]. Monoclonal antibodies against CTXs alone [3,47,115] or in combination with other therapies [117,118] could be considered in the future to prevent necrosis after a patient has been bitten by a snake in the *Naja* genus.

Similar results also showed no effective neutralization of progressive necrosis by the antivenom in the study by Dr. Liu et al. [82]. In our study, we clarified that CTXs played a major role in necrotic changes. We also highlighted that the venom was transported deeper to cause necrosis, although the dose was less than the MND and the antivenom agent was not effective based on the tissue biopsy scored by a veterinary pathologist.

Although the NET reaction was induced by the crude venom of *N. atra*, the role of NETs in the process of dermonecrosis is still unknown.

Although we individually removed the toxins in this study, we could not exclude the possibility of a synergistic effect of NTXs on necrosis. The antivenom concentration was unable to be increased in this animal experiment; however, in clinical practice, patients may respond to higher doses of antivenom.

Chapter 5 Conclusions

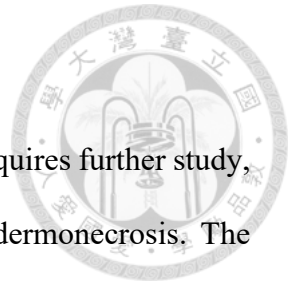


N. atra-related dermonecrosis may contribute to NET formation and the CTX effect.

Either the decorated granules on the NET or the trapped venom may exacerbate local damage. CTXs play a major role in *Naja atra* venom-induced necrosis. After the *N. atra* bite, even with the short fangs, the venom penetrated deeper rather than spreading along the surface. The deNTXs were distributed throughout the soft tissue rather than remaining localized at the site of injection, and severe damage was observed in the panniculus carnosus and adventitia. The antivenom did not prevent necrosis. The use of deNTXs allows mice to survive long enough to develop venom-induced cytolytic effects. In the future, management of *Naja atra* bites may include not only the existing antivenom to improve the survival rate but also the administration of monoclonal antibodies against CTXs or combined treatment with other therapies. The deNTX animal model is suitable for the purpose of these studies.

Chapter 6 Future perspectives

The mechanism of NET formation induced by *N. atra* venom requires further study, including the clinical effect of NETs on existing or diminishing dermonecrosis. The effectiveness of any potential therapy, such as monoclonal antibodies and decontamination, combined with antivenom is a possible trend in snakebite management in the future.



Chapter 7 List of publications



Year	Journal	Title	Authors
2021	Toxins 2021 Vol. 13 Issue 9 Pages 619-31	Analysis of the Necrosis-Inducing Components of the Venom of Naja atra and Assessment of the Neutralization Ability of Freeze-Dried Antivenom	<u>C.-H. Ho</u> , L.-C. Chiang, Y.-C. Mao, K.-C. Lan, S.-H. Tsai, Y.-J. Shih, et al.
2021	Clin Toxicol (Phila) 2021 Vol. 59 Issue 9 Pages 794-800	The role of a point-of-care ultrasound protocol in facilitating clinical decisions for snakebite envenomation in Taiwan: a pilot study	<u>C.-H. Ho</u> , A. K. Ismail, S. H. Liu, Y. S. Tzeng, L. Y. Li, F. C. Pai, et al.
2019	Journal of Medical Sciences 2019 Vol. 39 Issue 3 Pages 114-20	Descriptive study of snakebite patients in Northern Taiwan: 2009 to 2016	<u>C.-H. Ho</u> , Y.-C. Mao, Y.-D. Tsai, C.-S. Lin, S.-H. Liu, L.-C. Chiang, et al.



Figure 1 *Protobothrops mucrosquamatus* and *Naja atra*

The snake body. A 62-year-old male was bit by *P. mucrosquamatus* over the right thumb in 2018 (A) The gross dorsal view. (B) the Long Fang (arrow). A 62-year-old male was bit by *N. atra* over the right knee in 2016 (C) The gross ventral view. (D) the short fang (arrow) (E) cobra hood



Figure 2 *Protobothrops mucrosquamatus* related progress proximal edema

A 61-year-old male was bit by *Protobothrops mucrosquamatus* (identified by picture taken by the patient) in 2020. (A) Post bite 10 mins. Fang marker (arrow) (B) Post bite 2 hours, swelling progress to ankle (C) Post bite 4 hours, swelling progress to lower leg (D) Post bite 15 hours, progress to knee.



Figure 3 *Protobothrops mucrosquamatus* related dermonecrosis

A 62-year-old male, bitten by *P. mucrosquamatus* over his right thumb presented post bite 2.5 h. (B) Post bite 4.5 h. (C) Post bite 15 h. Bullae formation over right wrist and dorsal hand. (D) Post bite 22 h. (E) Post bite 2 weeks, dry gangrene was noted.

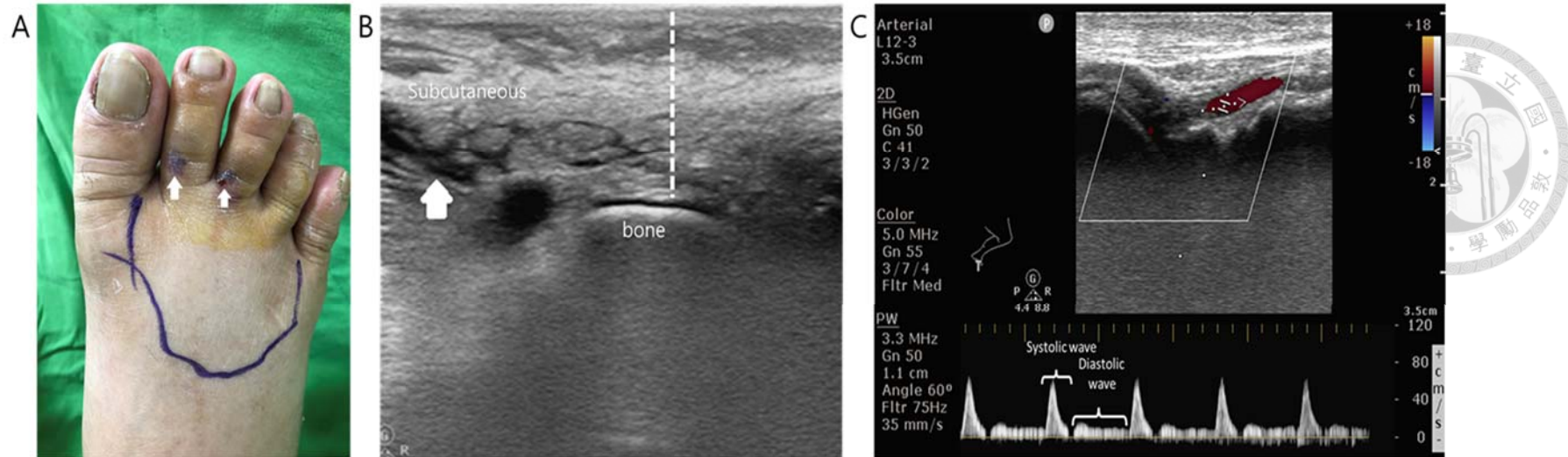


Figure 4 Point-of-care ultrasound (POCUS)

(A) The patient was bit by *Trimeresurus stejnegeri* with fang markers (Arrow) over the second and the third toes. (B) POCUS-The first method determined the location of edema. We used the relative locations of the cobblestone-like tissue and the fascia to evaluate whether the edema was in the fascia or the subcutaneous area. The cobblestone-like appearance (Arrow) located in the subcutaneous area (SCE). The dotted line means the separation of the cobblestone-like tissue and normal tissue. We marked the area to determine the rate of proximal swelling. (C) POCUS-The second method. We check the pulsed Doppler signal of the dorsalis pedis artery. Pulse wave tracing was performed with an angle of insonation less than 60 degrees over the target artery to identify the systolic and diastolic waves. Absence of diastolic retrograde arterial flow (DRAF) means the target artery is not compressed.

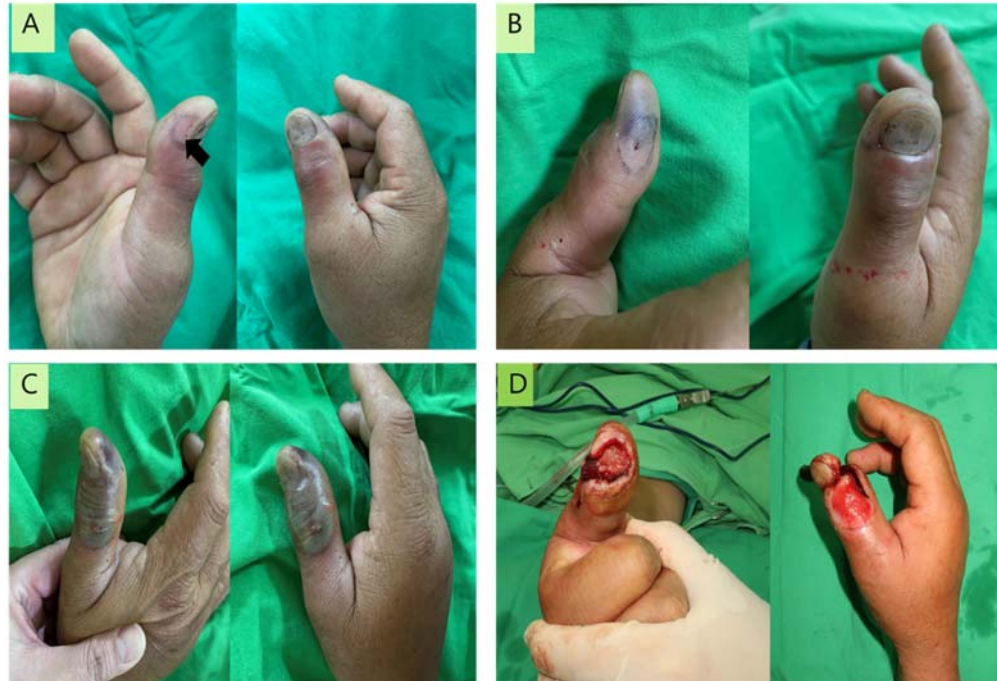


Figure 5 *Naja atra* dermonecrosis

A 51-year-old male was bitten over the right thumb distal phalanx by *N. atra*, which was identified by the patient. **(A)** Nine hours post-bite, the fang maker (arrow) was located over the radial side, and redness was located over the dorsal side of the thumb. **(B)** Fifteen hours post-bite, the necrotic change can be noted over the fang marker, and the redness is still noted over the dorsal side of the thumb. **(C)** Fifty-seven hours post-bite, the progress of necrosis was noted from the fang marker and progressing to dorsal side. **(D)** (Photo credits: *Yu-Jen Shih*) Ten days post-bite, the patient received the third time of debridement, and the necrotic tissue was all debrided and removed.

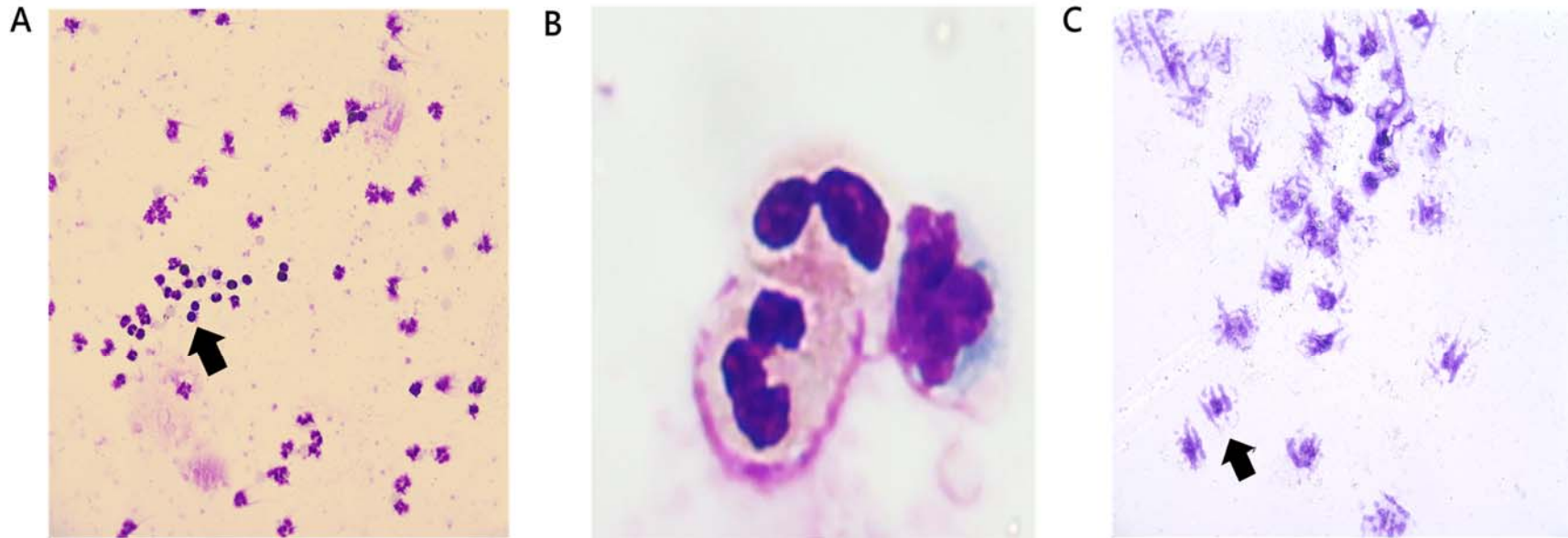


Figure 6 Neutrophil and Neutrophil extracellular trap

Isolated healthy adult neutrophil. (A) Neutrophil (arrow) had multiple lobe cellular nucleus (B) Isolated neutrophil (C) Isolated neutrophils mixed with PMA (phorbol 12-myristate 13-acetate) 4 hours later and released neutrophil extracellular trap (arrow). Wright and Giemsa stain. (C) Healthy neutrophil mixed with PBS (negative control), different concentration of *Naja atra* crude venom (1, 5 μ g/ml; 2, 25 μ g/ml; 3, 50 μ g/ml), P (PMA 100nM, positive control)

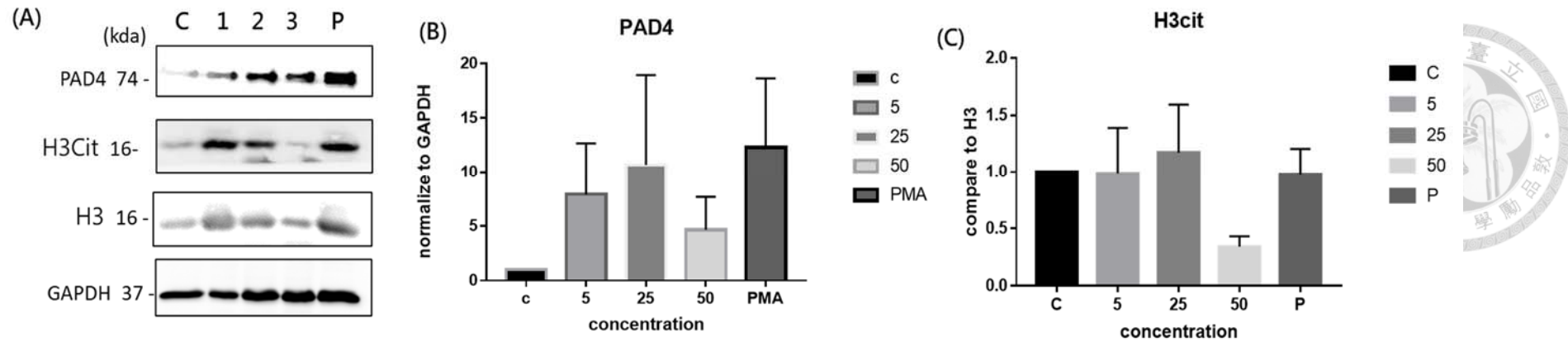


Figure 7 Western blot analysis of *Naja atra* related NET

(A) Western blot of healthy neutrophil mixed with PBS (C, negative control), different concentration of *Naja atra* crude venom (1, 5 $\mu\text{g/ml}$; 2, 25 $\mu\text{g/ml}$; 3, 50 $\mu\text{g/ml}$), P (PMA 100 nM, positive control) (B) PAD4 normalized to GAPDH (C) The ratio of H3Cit compares to H3

Abbreviation: PMA : Phorbol 12 myristate 13 acetate

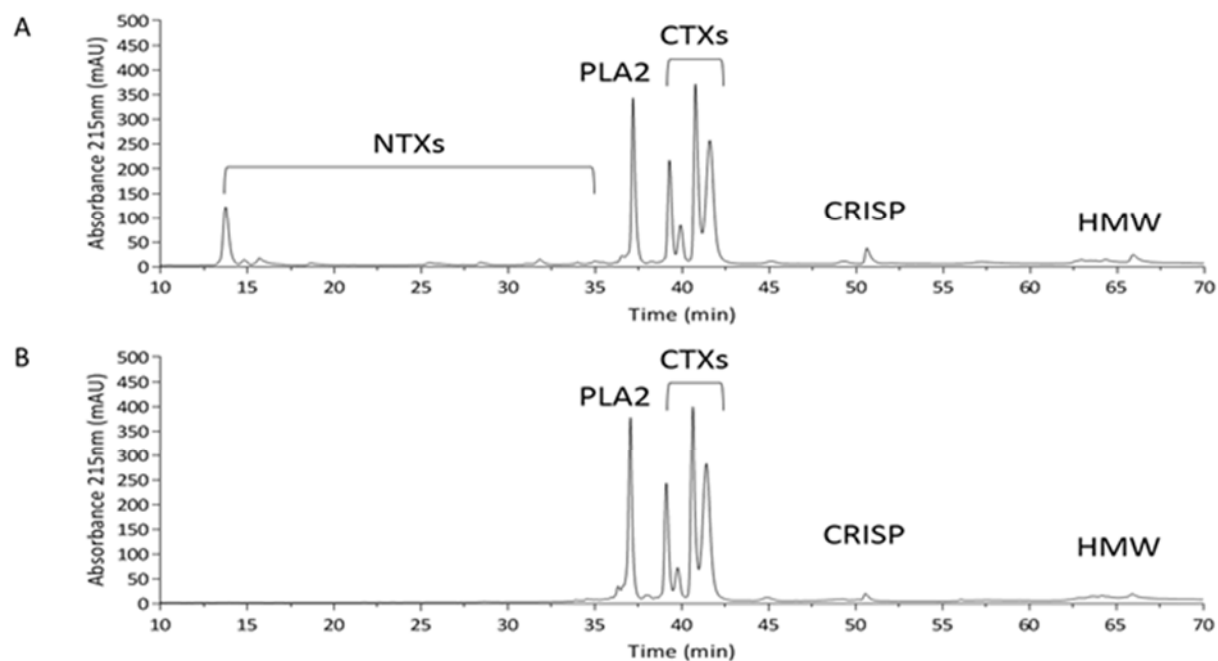


Figure 8 Characterization of *Naja atra* crude venom and crude venom devoid of NTXs.

HPLC profile of the *N. atra* crude venom sample and (B) *N. atra* crude venom devoid of NTXs (deNTXs). One hundred micrograms of both samples were applied to a Phenomenex Jupiter® C18 column (250 x 4.6 mm, 5 μ m particle size, 300 Å pore size) for analysis.

Abbreviation: NTXs, neurotoxins; PLA₂, phospholipase A₂; CTXs, cytotoxins also called cardiotoxins; CRISP, cysteine-rich secretory protein; HMW, high molecular weight proteins.

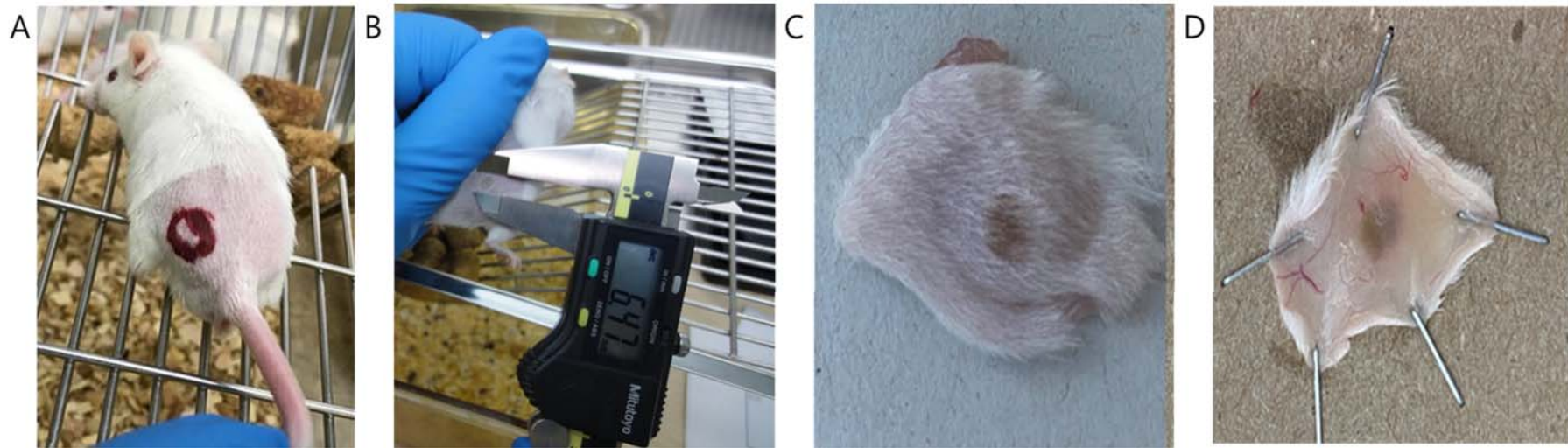


Figure 9 Intradermal injection with deNTXs *N. atra* venom

CD1 mice (10–12 weeks old) were grouped randomly (6 mice/group). The mice were injected intradermally with different levels (16.5, 20.5, 25.5, 32, and 40 μ g) of deNTXs *N. atra* venom after 72 hours. Measure the necrotic diameter more than 5 mm and determine the minimal necrosis dose with linear interpolation. (A, B) the dorsal skin hair removed and were intradermally injected with different venoms (C): Dorsal necrotic lesion (D): The inside of the necrotic lesion

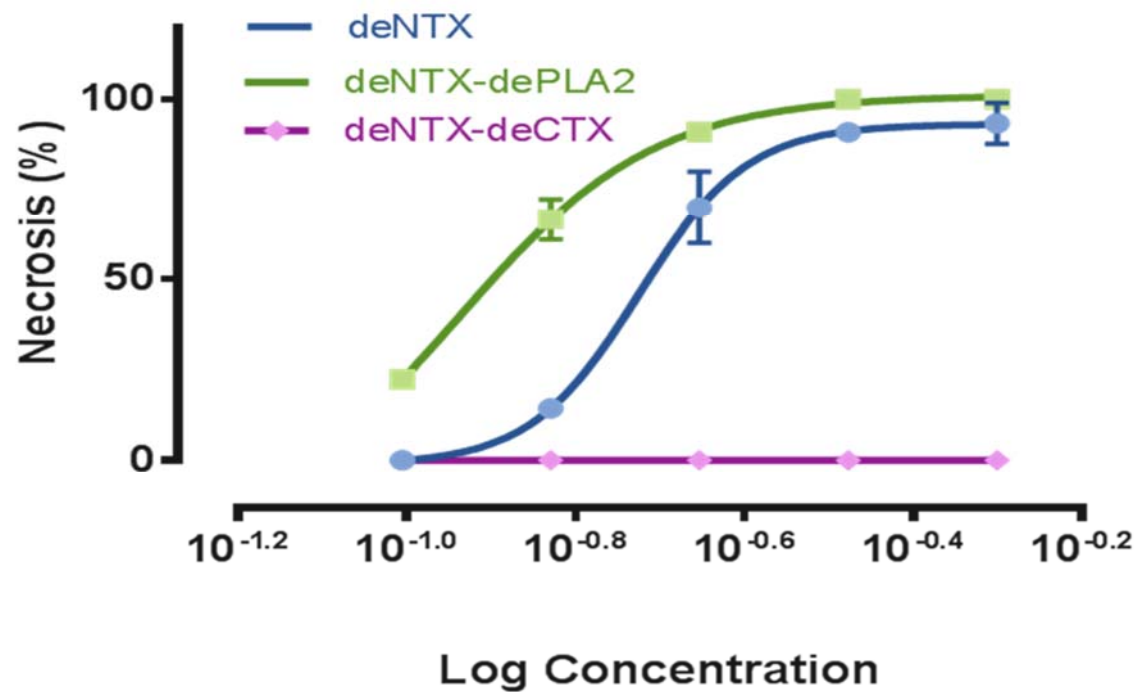


Figure 10 Minimal necrosis dose of different component of venom

deNTXs, blue curve; deNTXs-dePLA2, green curve; deNTXs-deCTX, purple curve.

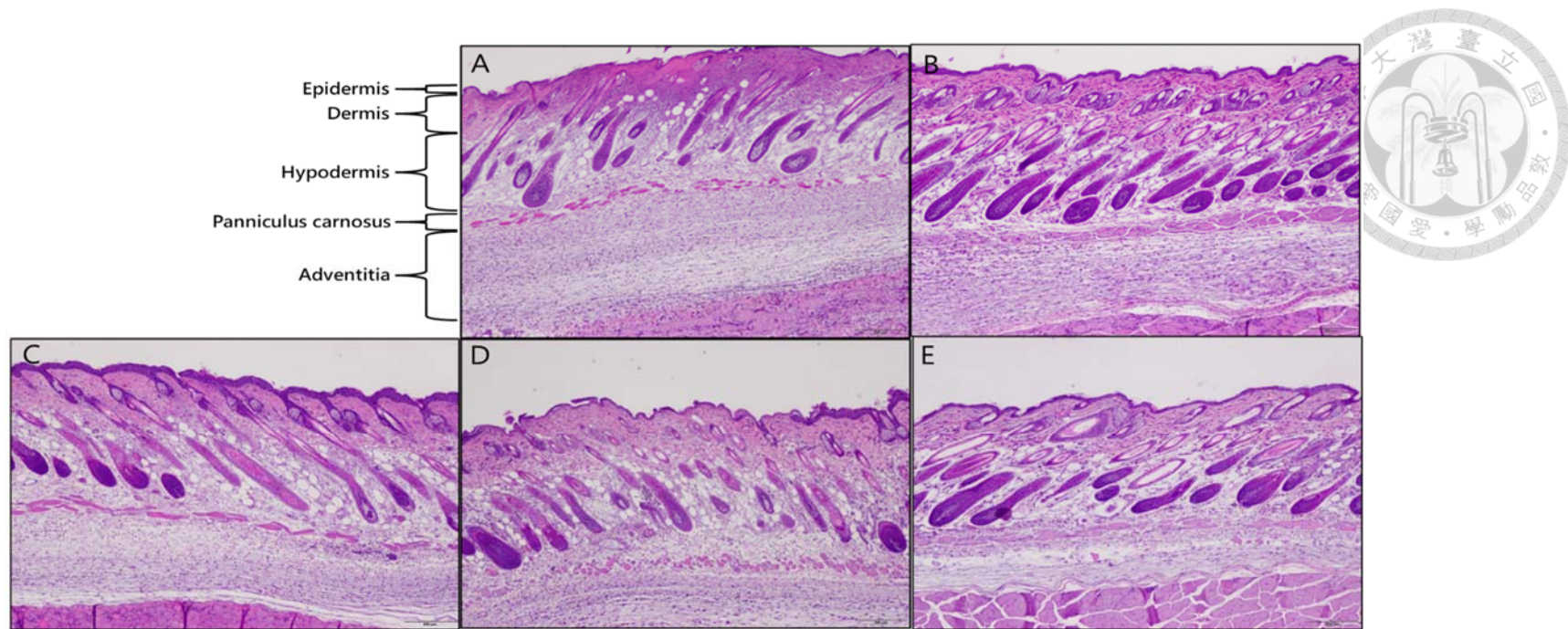


Figure 11 Skin biopsy of different levels of deNTXs *N. atra* venom

The mice (each group 6 mice) were injected intradermally over dermis/ hypodermis with different levels of venom of (A) 0.5, (B) 0.33, (C) 0.22, (D) 0.148, and (E) 0.098 $\mu\text{g/g}$ after 72 hours. The dorsal skin was removed and sent for skin biopsy with hematoxylin and eosin (HE) staining.

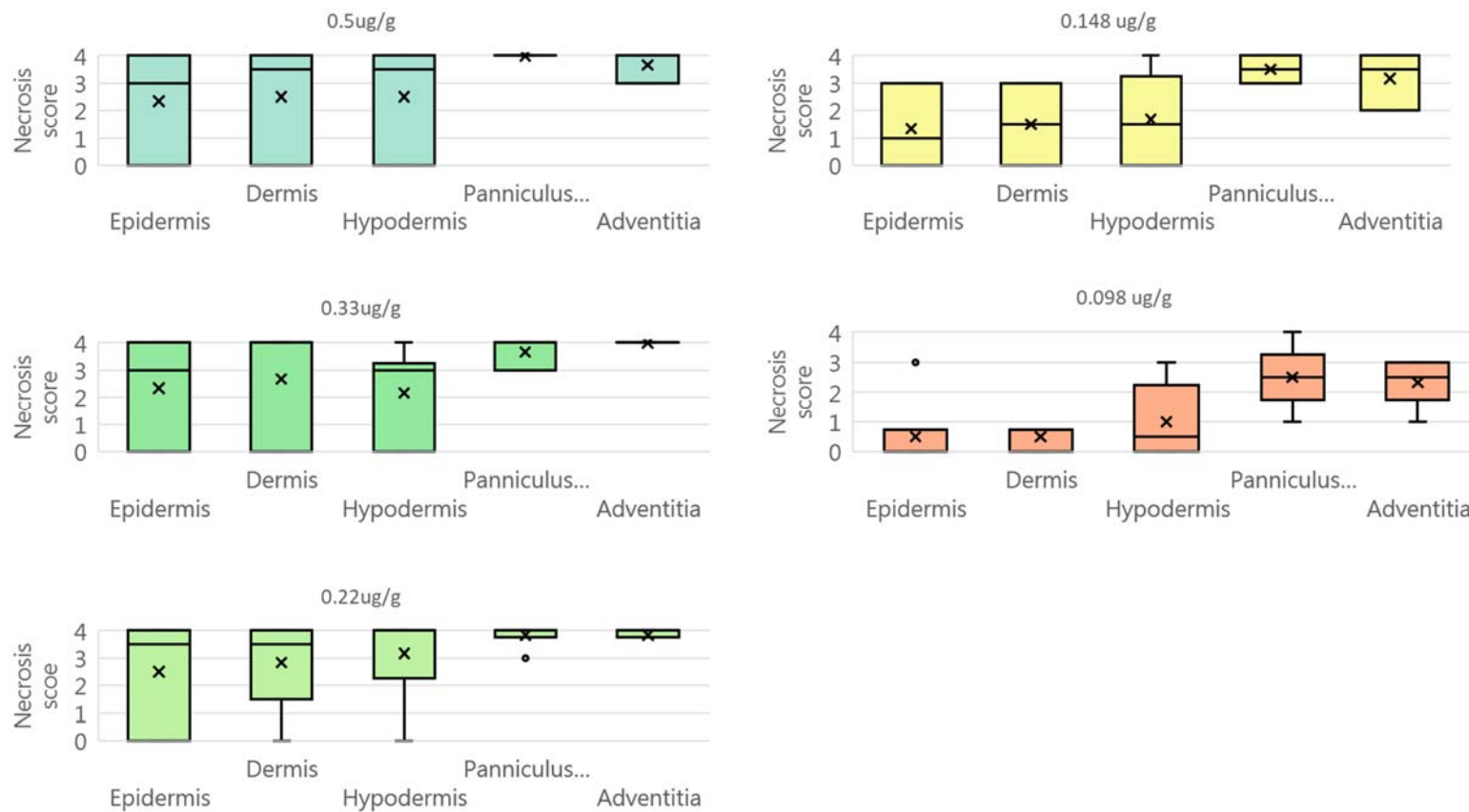


Figure 12 Tissue necrosis score of different levels of deNTXs *N. atra* venom

A veterinary pathologist scored the necrotic lesion layer by layer of the dorsal skin intradermally injected with different deNTXs doses (0.5; 0.33; 0.22; 0.148, and 0.098 $\mu\text{g/g}$) (each group 6 mice) three days later.

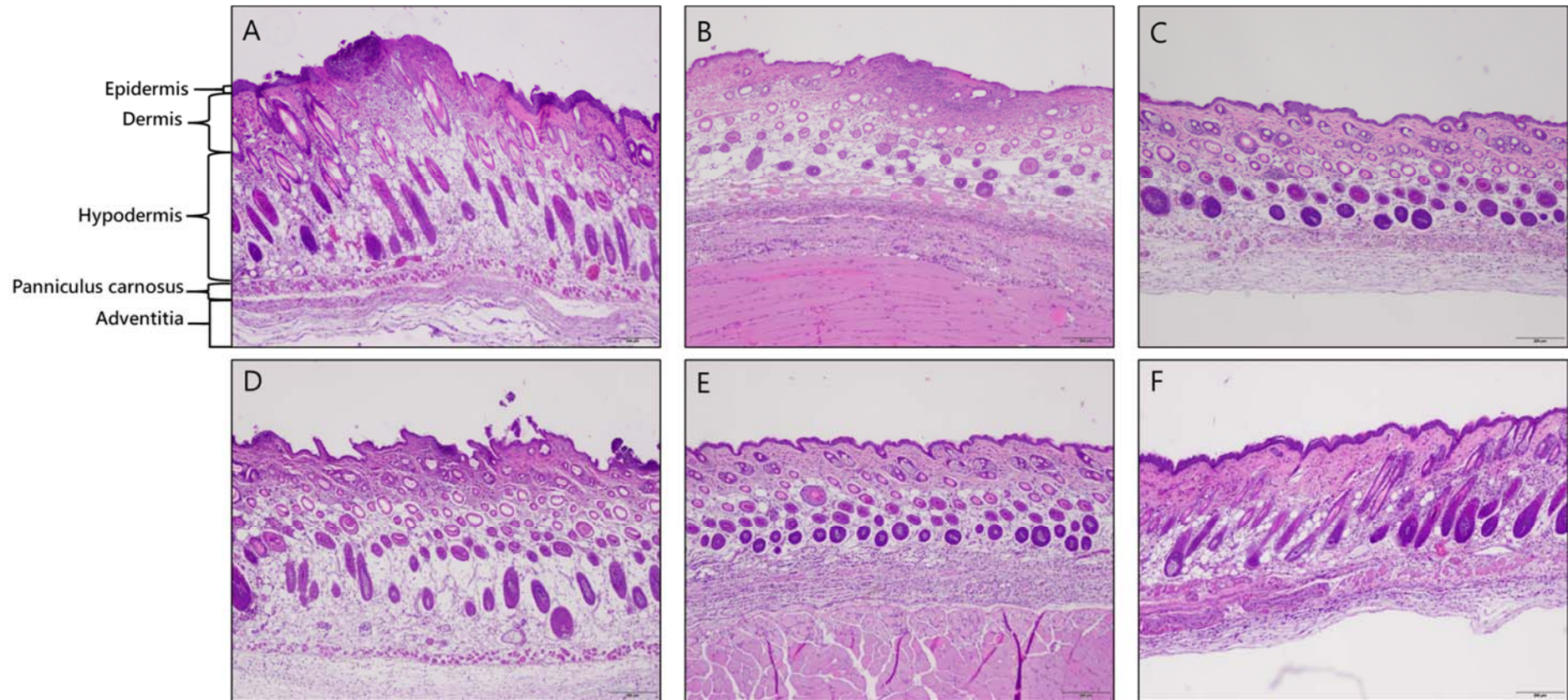


Figure 13 Skin biopsy of different dilutions of antivenom mixed with challenge dose

The mice (each group 5 mice) were injected intradermally with a mixture of the challenge dose (two times the MND of deNTXs) and different dilutions of antivenom (A, original; B 1:1; C 1:2; D 1:3; E 1:4; and F 1:5). The dorsal skin was removed and sent for skin biopsy with hematoxylin and eosin (HE) staining.

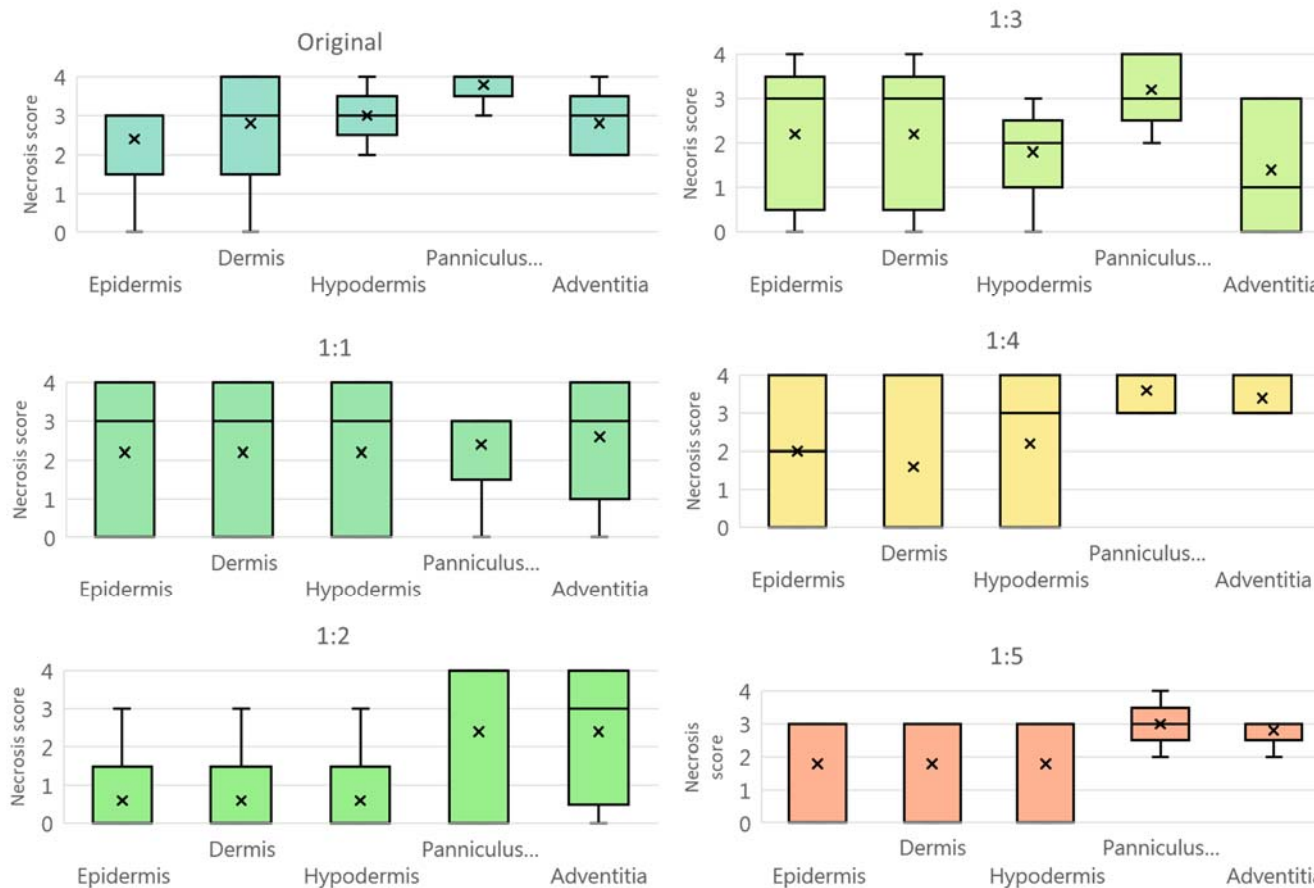


Figure 14 Tissue necrosis score of different dilutions of antivenom mixed with challenge dose

The mice (each group 5 mice) were injected intradermally with a mixture of the challenge dose (two times the MND of deNTXs) and different dilutions of antivenom (Original; 1:1; 1:2; 1:3; 1:4; and 1:5). After three days, the veterinary pathologist scored the necrotic lesion layer by layer of the dorsal skin.

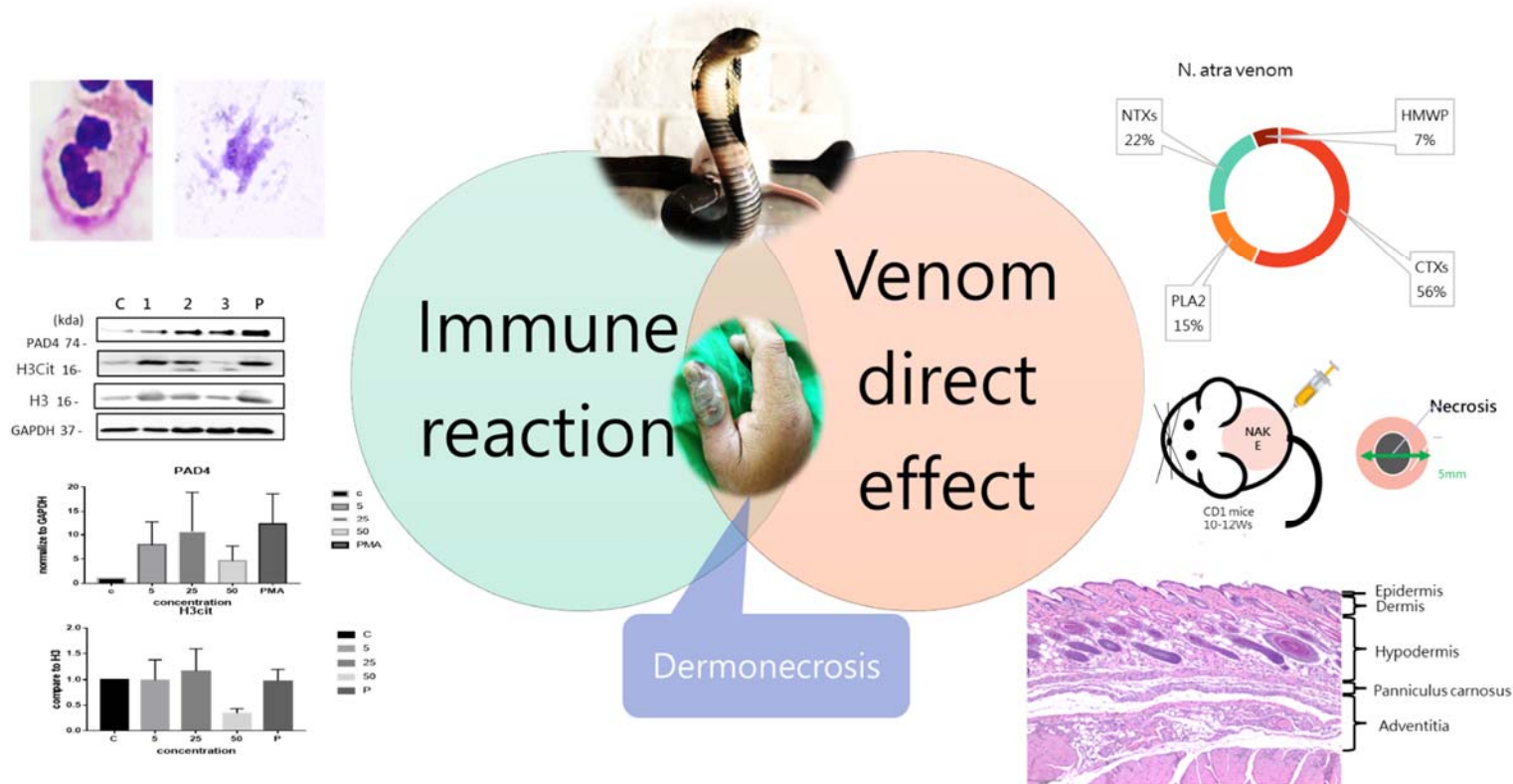


Figure 15 Graphical abstract

This study is to evaluate the mechanism of *N. atra* snakebite related dermonecrosis whether via the formation of NET and to clarify which is the major component of venom.

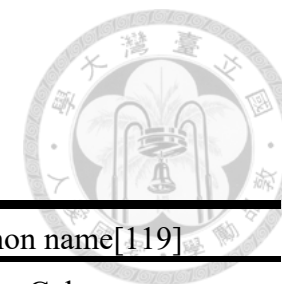


Table 1 Major species of venomous snakes in Taiwan

Family	Subfamily	Species	Regional Distribution	Common name[119]
Elapidae		<i>Naja atra</i>	Central Taiwan	Chinese Cobra
		<i>Bungarus multicinctus</i>	NA*	Many-banded Krait
Viperidae	Crotalinae	<i>Protobothrops mucrosquamatus</i>	Throughout the country, especially in the northern and southern areas	Taiwan Habu
		<i>Trimeresurus stejnegeri</i>		Green pit viper
		<i>stejnegeri</i>		
		<i>Deinagkistrodon acutus</i>	Hsinchu mountains	Hundred-Pacer
	Viperinae	<i>Daboia siamensis</i>	Southern and eastern Taiwan	Chain snake

* NA: non-available published data

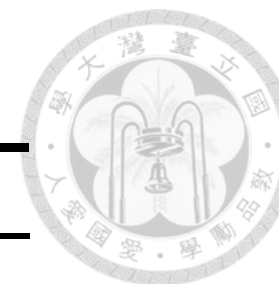


Table 2 Minimum necrotizing dose (MND) in different components of *Naja atra*

Name	Retained toxin	Concentration(mg/ml)	Toxin weight (μg)	MND (μg/g)
deNTXs	PLA ₂ , CTX, others [#]	0.198±0.012	9.88±0.576	0.494±0.029
deNTXs-dePLA ₂	CTX, others [#]	0.118±0.020	5.89±1.005	0.294±0.050
deNTXs-deCTXs	PLA ₂ , others [#]	>> 0.5	>>25	>>1.25

Abbreviations: NTX, neurotoxin; PLA₂, phospholipase A₂; CTX, cytotoxin also called cardiotoxin.

[#]: CRISP, cysteine-rich secretory protein; HMWP, high molecular weight proteins.



Table 3 Tissue necrosis score

Necrosis Score	Severity	Description
0	Normal	Within normal limits
1	Minimal	Sporadic occurrence
2	Mild	Aggregated distribution
3	Moderate	Regional distribution
4	Severe	Diffuse distribution and lose originality



Table 4 Necrosis scores with different deNTXs doses (each group contained six mice)

deNTXs dosage	0.5 µg/g (P: 0.168)						0.33 µg/g (P: 0.058)						0.22 µg/g (P: 0.0443)						0.148 µg/g * (*P: 0.038)						0.098 µg/g * (*P: 0.013)						
Epidermis	3	0	4	0	4	3	4	4	3	3	0	0	3	4	4	0	0	4	3	3	0	0	2	0	0	0	0	3	0	0	
Dermis	3	0	4	0	4	4	4	4	4	4	0	0	3	4	4	0	2	4	3	3	0	0	3	0	0	0	0	3	0	0	
Hypodermis	3	0	4	0	4	4	4	3	3	3	0	0	4	4	4	0	3	4	4	3	0	0	3	0	0	0	0	3	2	1	
Panniculus carnosus	4	4	4	4	4	4	4	4	4	4	3	3	4	4	3	4	4	4	4	3	3	3	3	4	4	3	3	1	4	2	2
Adventitia	3	3	4	4	4	4	4	4	4	4	4	4	4	4	4	3	4	4	4	3	2	2	4	4	2	2	1	3	3	3	

Kruskal-Wallis test



Table 5 Necrosis scores under a fixed challenge dose (2MND) mixed with different dilution times of antivenom (AV)
(Each group contains five mice)

Antivenom	A1 (P: 0.153)					A2 (P: 0.991)					A3 (P: 0.109)					A4 (P: 0.307)					A5 (P: 0.573)					A6 (P: 0.567)				
Epidermis	3	0	3	3	3	3	0	4	4	0	0	3	0	0	0	4	3	3	1	0	0	4	4	2	0	0	3	3	0	3
Dermis	3	0	4	3	4	3	0	4	4	0	0	3	0	0	0	4	3	3	1	0	0	4	4	0	0	0	3	3	0	3
Hypodermis	3	2	3	3	4	3	0	4	4	0	0	3	0	0	0	2	3	2	2	0	0	4	4	3	0	0	3	3	0	3
Panniculus carnosus	4	4	4	4	3	3	0	3	3	3	0	0	4	4	4	2	4	4	3	3	4	3	3	4	4	2	3	3	4	3
Adventitia	2	2	4	3	3	2	0	4	4	3	0	1	4	4	3	0	0	1	3	3	3	4	4	3	3	2	3	3	3	3

A1: original AV concentration; A2: 1:1 dilution; A3 1:2 dilution; A4 1:3 dilution; A5 1:4 dilution; A6 1:5 dilution

Kruskal-Wallis test



Table 6 Comparison between the LD₅₀ and minimum necrotizing dose

	Crude venom	NTX	PLA2	CTX	Others ¹	Reference
Average composition ratio (%)		22.0	15.4	56.2	6.5	[79]
LD ₅₀ (μg/g)	0.56 (iv.)	0.075 (iv.)	NA	NA	NA	[97]
Devoid different composition venom						
MND (μg/g)	0.494±0.029 (id.)	Devoid				
	0.294±0.050 (id.)	Devoid	Devoid			
	>>1.25(id.)	Devoid		Devoid		

Abbreviations: NTX, neurotoxin; PLA2, phospholipase A₂; CTX, cytotoxin also called cardiotoxin; iv., Intravenous route; id., intradermal; NA, non-available

¹: CRISP, cysteine-rich secretory protein and high molecular weight proteins



Table 7 Taiwan Antivenom and Recommend doses

Antivenom	PCC*recommend[3]
Antivenin of <i>Bungarus multicinctus</i> and <i>Naja naja atra</i>	2–4 vials for <i>B. multicinctus</i> 6–10 vials for <i>N. atra</i>
Antivenin of <i>Trimeresurus mucrosquamatus</i> [#] and <i>Trimeresurus gramineus</i>	1-2 vials for <i>Trimeresurus stejnegeri stejnegeri</i> 2-4 vials for <i>Protobothrops mucrosquamatus</i>
Antivenin of <i>Daboia russellii</i>	2–4 vials
Antivenin of <i>Deinagkistrodon acutus</i>	2–4 vials

the species corrected to *Protobothrops mucrosquamatus*, *Trimeresurus stejnegeri stejnegeri*

* PCC-Taiwan: Taiwan's National Poison Control Center

References



1. Mao Y-C, Hung D-Z. Epidemiology of Snake Envenomation in Taiwan. In: Gopalakrishnakone P, editor. Clinical Toxinology in Asia Pacific and Africa. 1 ed. New York Dordrecht London: Springer Heidelberg 2015. p. 3-22.
2. Hung DZ. Taiwan's venomous snakebite: epidemiological, evolution and geographic differences. Transactions of the Royal Society of Tropical Medicine and Hygiene. 2004 Feb;98(2):96-101.
3. Mao Y-C, Hung D-Z. Management of Snake Envenomation in Taiwan. In: Gopalakrishnakone P, editor. Clinical Toxinology in Asia Pacific and Africa, Toxinology. 1 ed. Heidelberg New York Dordrecht London: Springer 2015. p. 23-52.
4. Ho C-H, Mao Y-C, Tsai Y-D, et al. Descriptive study of snakebite patients in Northern Taiwan: 2009 to 2016. Journal of Medical Sciences. 2019;39(3):114-120.
5. Mao YC, Liu PY, Chiang LC, et al. Naja atra snakebite in Taiwan. Clin Toxicol (Phila). 2017 Aug 23:273-80.
6. Mao YC, Liu PY, Chiang LC, et al. Clinical manifestations and treatments of Protobothrops mucrosquamatus bite and associated factors for wound necrosis and subsequent debridement and finger or toe amputation surgery. Clin Toxicol (Phila). 2020 May 13:28-37.
7. Torlincasi AM, Lopez RA, Waseem M. Acute Compartment Syndrome. StatPearls. Treasure Island (FL): StatPearls Publishing Copyright © 2021, StatPearls Publishing LLC.; 2021. p. 1-4.
8. Turkmen A, Temel M. Algorithmic approach to the prevention of unnecessary

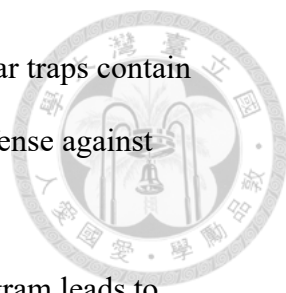
- fasciotomy in extremity snake bite. *Injury*. 2016 Dec;47(12):2822-2827.
9. Andrea Stracciolini M, Mark Hammerberg M. Acute compartment syndrome of the extremities UpToDate2018 [updated Apr 18, 2018.]. Available from: <https://www.uptodate.com/contents/acute-compartment-syndrome-of-the-extremities>
10. Hsieh YH, Hsueh JH, Liu WC, et al. Contributing Factors for Complications and Outcomes in Patients With Snakebite: Experience in a Medical Center in Southern Taiwan. *Annals of plastic surgery*. 2017 Mar;78(3 Suppl 2):S32-6.
11. Chang KP, Lai CS, Lin SD. Management of poisonous snake bites in southern Taiwan. *The Kaohsiung journal of medical sciences*. 2007 Oct;23(10):511-8.
12. Chen JC, Liaw SJ, Bullard MJ, et al. Treatment of poisonous snakebites in northern Taiwan. *J Formos Med Assoc*. 2000 Feb;99(2):135-9.
13. Kanaan NC, Ray J, Stewart M, et al. Wilderness Medical Society Practice Guidelines for the Treatment of Pitviper Envenomations in the United States and Canada. *Wilderness & environmental medicine*. 2015 Dec;26(4):472-87.
14. Cumpston KL. Is there a role for fasciotomy in Crotalinae envenomations in North America? *Clin Toxicol (Phila)*. 2011 Jun;49(5):351-65.
15. Halanski MA, Morris MR, Lee Harper B, et al. Intracompartmental Pressure Monitoring Using a Handheld Pressure Monitoring System. *JBJS Essent Surg Tech*. 2015;5(1):e171-5.
16. STIC Intra-Compartmental Pressure Monitor [Internet]2021. Available from: <https://c2dx.co/products/stic-pressure-monitor/>.
17. Intracompartmental Pressures [Internet]. Available from: <https://millar.com/Clinical/Clinical-Applications/Intracompartmental-Pressures/>.
18. Hammerberg EM, Whitesides TE, Jr., Seiler JG, 3rd. The reliability of

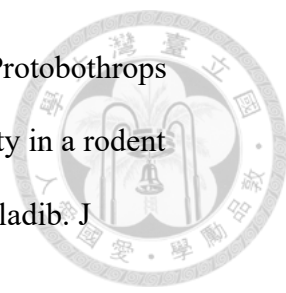
- measurement of tissue pressure in compartment syndrome. *Journal of orthopaedic trauma*. 2012 Sep;26(9):24-32.
19. Ho CH, Ismail AK, Liu SH, et al. The role of a point-of-care ultrasound protocol in facilitating clinical decisions for snakebite envenomation in Taiwan: a pilot study. *Clin Toxicol (Phila)*. 2021 Sep;59(9):794-800.
20. Mc Loughlin S, Mc Loughlin MJ, Mateu F. Pulsed Doppler in simulated compartment syndrome: a pilot study to record hemodynamic compromise. *Ochsner J*. 2013 Winter;13(4):500-6.
21. Gutierrez JM, Calvete JJ, Habib AG, et al. Snakebite envenoming. *Nature reviews Disease primers*. 2017 Sep 14;3:1-20.
22. Jimenez-Alcazar M, Rangaswamy C, Panda R, et al. Host DNases prevent vascular occlusion by neutrophil extracellular traps. *Science (New York, NY)*. 2017 Dec 1;358(6367):1202-6.
23. Katkar GD, Sundaram MS, NaveenKumar SK, et al. NETosis and lack of DNase activity are key factors in *Echis carinatus* venom-induced tissue destruction. *Nature communications*. 2016 Apr 19;7:1-13.
24. Noutsos T, Currie BJ, Isbister GK. Snakebite associated thrombotic microangiopathy: a protocol for the systematic review of clinical features, outcomes, and role of interventions. *Syst Rev*. 2019 Aug 22;8(1):s13643-019.
25. Mao YC, Liu PY, Hung DZ, et al. Bacteriology of *Naja atra* Snakebite Wound and Its Implications for Antibiotic Therapy. *The American journal of tropical medicine and hygiene*. 2016 May 04;94(5):1129-35.
26. Ghose A, White J. Asian Snakes. *Critical Care Toxicology* 2017. p. 2343-2403.
27. Warrell DA. Snake bite. *The Lancet*. 2010 2010/01/02/;375(9708):77-88.
28. Rivel M, Solano D, Herrera M, et al. Pathogenesis of dermonecrosis induced by

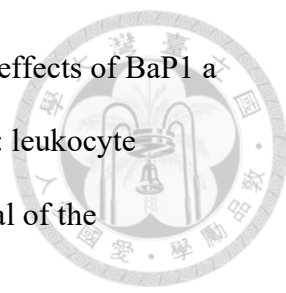
venom of the spitting cobra, *Naja nigricollis*: An experimental study in mice.

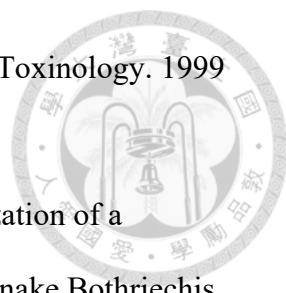
Toxicon : official journal of the International Society on Toxinology. 2016 Sep 1;119:171-9.

29. Warrell DA, Greenwood BM, Davidson NM, et al. Necrosis, haemorrhage and complement depletion following bites by the spitting cobra (*Naja nigricollis*). Q J Med. 1976 Jan;45(177):1-22.
30. Iddon D, Theakston RD, Ownby CL. A study of the pathogenesis of local skin necrosis induced by *Naja nigricollis* (spitting cobra) venom using simple histological staining techniques. Toxicon : official journal of the International Society on Toxinology. 1987;25(6):665-72.
31. Zuliani JP, Soares AM, Gutiérrez JM. Polymorphonuclear neutrophil leukocytes in snakebite envenoming. Toxicon : official journal of the International Society on Toxinology. 2020 Nov;187:188-97.
32. Gutiérrez JM, Chaves F, Cerdas L. Inflammatory infiltrate in skeletal muscle injected with *Bothrops asper* venom. Rev Biol Trop. 1986 Nov;34(2):209-14.
33. Liew PX, Kubes P. The Neutrophil's Role During Health and Disease. Physiol Rev. 2019 Apr 1;99(2):1223-48.
34. Hickey MJ, Kubes P. Intravascular immunity: the host-pathogen encounter in blood vessels. Nature reviews Immunology. 2009 May;9(5):364-75.
35. Mortaz E, Alipoor SD, Adcock IM, et al. Update on Neutrophil Function in Severe Inflammation. Front Immunol. 2018;9:1-14.
36. Brinkmann V, Reichard U, Goosmann C, et al. Neutrophil extracellular traps kill bacteria. Science (New York, NY). 2004 Mar 5;303(5663):1532-5.
37. Papayannopoulos V. Neutrophil extracellular traps in immunity and disease. Nature reviews Immunology. 2018 Feb;18(2):134-47.

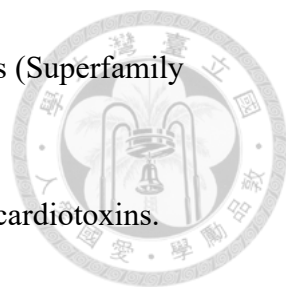
- 
38. Urban CF, Ermert D, Schmid M, et al. Neutrophil extracellular traps contain calprotectin, a cytosolic protein complex involved in host defense against *Candida albicans*. *PLoS pathogens*. 2009 Oct;5(10):1-18.
39. Fuchs TA, Abed U, Goosmann C, et al. Novel cell death program leads to neutrophil extracellular traps. *J Cell Biol*. 2007 Jan 15;176(2):231-41.
40. Pilsczek FH, Salina D, Poon KK, et al. A novel mechanism of rapid nuclear neutrophil extracellular trap formation in response to *Staphylococcus aureus*. *Journal of immunology (Baltimore, Md : 1950)*. 2010 Dec 15;185(12):7413-25.
41. Yipp BG, Petri B, Salina D, et al. Infection-induced NETosis is a dynamic process involving neutrophil multitasking in vivo. *Nat Med*. 2012 Sep;18(9):1386-93.
42. Mutua V, Gershwin LJ. A Review of Neutrophil Extracellular Traps (NETs) in Disease: Potential Anti-NETs Therapeutics. *Clin Rev Allergy Immunol*. 2021 Oct;61(2):194-211.
43. Dunbar JP, Sulpice R, Dugon MM. The kiss of (cell) death: can venom-induced immune response contribute to dermal necrosis following arthropod envenomations? *Clin Toxicol (Phila)*. 2019 Aug;57(8):677-85.
44. Xu Y-L, Kou J-Q, Wang S-Z, et al. Neurotoxin from *Naja naja atra* venom inhibits skin allograft rejection in rats. *International Immunopharmacology*. 2015;28(1):188-98.
45. Standker L, Harvey AL, Furst S, et al. Improved method for the isolation, characterization and examination of neuromuscular and toxic properties of selected polypeptide fractions from the crude venom of the Taiwan cobra *Naja naja atra*. *Toxicon : official journal of the International Society on Toxinology*. 2012 Sep 15;60(4):623-31.

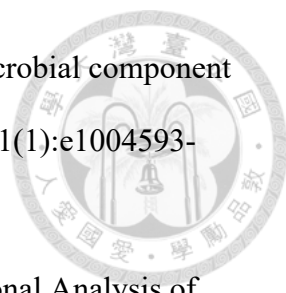
- 
46. Liu CC, Wu CJ, Hsiao YC, et al. Snake venom proteome of *Protobothrops mucrosquamatus* in Taiwan: Delaying venom-induced lethality in a rodent model by inhibition of phospholipase A2 activity with varespladib. *J Proteomics*. 2021 Mar 15;234:104084-93.
47. Huang HW, Liu BS, Chien KY, et al. Cobra venom proteome and glycome determined from individual snakes of *Naja atra* reveal medically important dynamic range and systematic geographic variation. *J Proteomics*. 2015 Oct 14;128:92-104.
48. Sun QY, Bao J. Purification, cloning and characterization of a metalloproteinase from *Naja atra* venom. *Toxicon : official journal of the International Society on Toxinology*. 2010 Dec;56(8):1459-69.
49. Guan HH, Goh KS, Davamani F, et al. Structures of two elapid snake venom metalloproteases with distinct activities highlight the disulfide patterns in the D domain of ADAMalysin family proteins. *J Struct Biol*. 2010 Mar;169(3):294-303.
50. Li R, Zhu S, Wu J, et al. L-amino acid oxidase from *Naja atra* venom activates and binds to human platelets. *Acta Biochim Biophys Sin (Shanghai)*. 2008 Jan;40(1):19-26.
51. Tan NH, Saifuddin MN. Isolation and characterization of a hemorrhagin from the venom of *Ophiophagus hannah* (king cobra). *Toxicon : official journal of the International Society on Toxinology*. 1990;28(4):385-92.
52. José María Gutiérrez, Alexandra Rucavado, Escalante T. Snake Venom Metalloproteinases Biological Roles and Participation in the Pathophysiology of Envenomation. In: Mackessy SP, Mackessy SP, editors. *Handbook of Venoms and Toxins of Reptiles* 2009. p. 115-39.

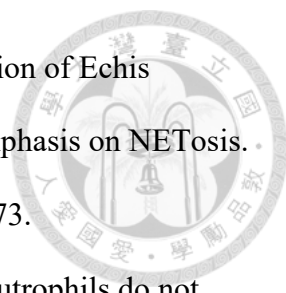
- 
53. Fernandes CM, Zamuner SR, Zuliani JP, et al. Inflammatory effects of BaP1 a metalloproteinase isolated from Bothrops asper snake venom: leukocyte recruitment and release of cytokines. *Toxicon : official journal of the International Society on Toxinology*. 2006 Apr;47(5):549-59.
54. Laing GD, Clissa PB, Theakston RD, et al. Inflammatory pathogenesis of snake venom metalloproteinase-induced skin necrosis. *Eur J Immunol*. 2003 Dec;33(12):3458-63.
55. Rucavado A, Escalante T, Teixeira CF, et al. Increments in cytokines and matrix metalloproteinases in skeletal muscle after injection of tissue-damaging toxins from the venom of the snake *Bothrops asper*. *Mediators Inflamm*. 2002 Apr;11(2):121-8.
56. Dennis EA. Diversity of group types, regulation, and function of phospholipase A2. *J Biol Chem*. 1994 May 6;269(18):13057-60.
57. Robin Doley, Xingding Zhou, Kini RM. Snake Venom Phospholipase A2 Enzymes. In: Stephen P. Mackessy, Mackessy SP, editors. *Handbook of Venoms and Toxins of Reptiles*. Boca Raton 2009. p. 173-207.
58. Six DA, Dennis EA. The expanding superfamily of phospholipase A(2) enzymes: classification and characterization. *Biochim Biophys Acta*. 2000 Oct 31;1488(1-2):1-19.
59. Murakami MT, Gabdoulkhakov A, Genov N, et al. Insights into metal ion binding in phospholipases A2: ultra high-resolution crystal structures of an acidic phospholipase A2 in the Ca²⁺ free and bound states. *Biochimie*. 2006 May;88(5):543-9.
60. Ali SA, Alam JM, Stoeva S, et al. Sea snake *Hydrophis cyanocinctus* venom. I. Purification, characterization and N-terminal sequence of two phospholipases

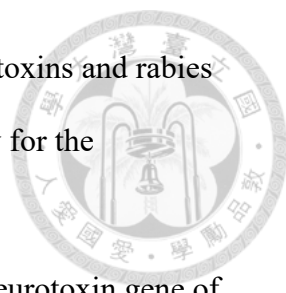
- 
- A2. Toxicon : official journal of the International Society on Toxinology. 1999 Nov;37(11):1505-20.
61. Angulo Y, Chaves E, Alape A, et al. Isolation and characterization of a myotoxic phospholipase A2 from the venom of the arboreal snake *Bothriechis (Bothrops) schlegelii* from Costa Rica. Arch Biochem Biophys. 1997 Mar 15;339(2):260-6.
62. Kini RM, Evans HJ. A model to explain the pharmacological effects of snake venom phospholipases A2. Toxicon : official journal of the International Society on Toxinology. 1989;27(6):613-35.
63. Freedman JE, Snyder SH. Vipoxin. A protein from Russell's viper venom with high affinity for biogenic amine receptors. J Biol Chem. 1981 Dec 25;256(24):13172-9.
64. Jiang MS, Fletcher JE, Smith LA. Effects of divalent cations on snake venom cardiotoxin-induced hemolysis and 3H-deoxyglucose-6-phosphate release from human red blood cells. Toxicon : official journal of the International Society on Toxinology. 1989;27(12):1297-305.
65. Huang MZ, Wang QC, Liu GF. Effects of an acidic phospholipase A2 purified from *Ophiophagus hannah* (king cobra) venom on rat heart. Toxicon : official journal of the International Society on Toxinology. 1993 May;31(5):627-35.
66. Gutiérrez JM, Ownby CL. Skeletal muscle degeneration induced by venom phospholipases A2: insights into the mechanisms of local and systemic myotoxicity. Toxicon : official journal of the International Society on Toxinology. 2003 Dec 15;42(8):915-31.
67. Gasanov SE, Dagda RK, Rael ED. Snake Venom Cytotoxins, Phospholipase A(2)s, and Zn(2+)-dependent Metalloproteinases: Mechanisms of Action and

- Pharmacological Relevance. Journal of clinical toxicology. 2014;4(1):1000181-215.
68. Montecucco C, Gutiérrez JM, Lomonte B. Cellular pathology induced by snake venom phospholipase A2 myotoxins and neurotoxins: common aspects of their mechanisms of action. Cell Mol Life Sci. 2008 Sep;65(18):2897-912.
69. Hiu JJ, Yap MKK. Cytotoxicity of snake venom enzymatic toxins: phospholipase A2 and l-amino acid oxidase. Biochem Soc Trans. 2020 Apr 29;48(2):719-31.
70. Ebrahim K, Shirazi FH, Mirakabadi AZ, et al. Cobra venom cytotoxins; apoptotic or necrotic agents? Toxicon : official journal of the International Society on Toxinology. 2015 Dec 15;108:134-40.
71. Raghurama P. Hegde, Nandhakishore Rajagopalan, Robin Doley, et al. Snake Venom Three-Finger Toxins In: Mackessy SP, Mackessy SP, editors. Handbook of Venoms and Toxins of Reptiles 2009. p. 287-303.
72. Tsetlin V. Snake venom alpha-neurotoxins and other 'three-finger' proteins. Eur J Biochem. 1999 Sep;264(2):281-6.
73. Ménez A. Functional architectures of animal toxins: a clue to drug design? Toxicon : official journal of the International Society on Toxinology. 1998 Nov;36(11):1557-72.
74. Pahari S, Bickford D, Fry BG, et al. Expression pattern of three-finger toxin and phospholipase A2 genes in the venom glands of two sea snakes, *Lapemis curtus* and *Acalyptophis peronii*: comparison of evolution of these toxins in land snakes, sea kraits and sea snakes. BMC Evol Biol. 2007 Sep 27;7:175-84.
75. Pahari S, Mackessy SP, Kini RM. The venom gland transcriptome of the Desert Massasauga rattlesnake (*Sistrurus catenatus edwardsii*): towards an

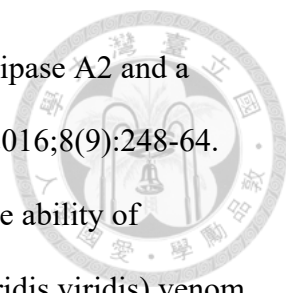
- 
- understanding of venom composition among advanced snakes (Superfamily Colubroidea). BMC Mol Biol. 2007 Dec 20;8:115-32.
76. Boffa MC, Barbier D, de Angulo M. Anticoagulant effect of cardiotoxins. Thromb Res. 1983 Dec 15;32(6):635-40.
77. Dubovskii PV, Konshina AG, Efremov RG. Cobra cardiotoxins: membrane interactions and pharmacological potential. Curr Med Chem. 2014;21(3):270-87.
78. Wu M, Ming W, Tang Y, et al. The anticancer effect of cytotoxin 1 from *Naja atra* Cantor venom is mediated by a lysosomal cell death pathway involving lysosomal membrane permeabilization and cathepsin B release. Am J Chin Med. 2013;41(3):643-63.
79. Huang RJ, Chen SW, Chen TK, et al. [The detoxification of *Naja naja atra* venom and preparation of potent antivenin]. Zhonghua Min Guo Wei Sheng Wu Ji Mian Yi Xue Za Zhi. 1985 Aug;18(3):177-83.
80. Chien-Hsin Liu, Chia-jung Lee, Rung Li, et al. Application of Snake-Venom and Technology of Antivenom Manufactory. Taiwan Epidemiology Bulletin. 2015:76-86.
81. WHO Expert Committee on Biological Standardization, sixty-seventh report. Geneva: World Health Organization; 2017 (WHO technical report series ; no. 1004). In: Organization WH, editor. 2017. p. 321-2.
82. Liu CC, Chou YS, Chen CY, et al. Pathogenesis of local necrosis induced by *Naja atra* venom: Assessment of the neutralization ability of Taiwanese freeze-dried neurotoxic antivenom in animal models. PLoS neglected tropical diseases. 2020 Feb;14(2):e0008054-74.
83. 徐亞莉、吳佳蓉、周祖楨、謝文欽、鄭雅芬、江正榮. 台灣抗蛇毒血清製造之回顧與展望. 2013:64-78.

- 
84. Halverson TW, Wilton M, Poon KK, et al. DNA is an antimicrobial component of neutrophil extracellular traps. *PLoS pathogens*. 2015 Jan;11(1):e1004593-616.
 85. Kuhns DB, Long Priel DA, Chu J, et al. Isolation and Functional Analysis of Human Neutrophils. *Current protocols in immunology*. 2015 Nov 02;111:7.23.1-16.
 86. Wong SL, Demers M, Martinod K, et al. Diabetes primes neutrophils to undergo NETosis, which impairs wound healing. *Nat Med*. 2015 Jul;21(7):815-9.
 87. Chen KC, Lin AC, Chong CF, et al. An overview of point-of-care ultrasound for soft tissue and musculoskeletal applications in the emergency department. *J Intensive Care*. 2016;4:55-66.
 88. Vohra R, Rangan C, Bengiamin R. Sonographic signs of snakebite. *Clin Toxicol (Phila)*. 2014 Nov;52(9):948-51.
 89. Sivaganabalan R, Ismail AK, Salleh M, et al. QUICK GUIDE ON SNAKEBITE MANAGEMENT FOR HEALTHCARE PROVIDERS IN MALAYSIA. 2017. p. 1-10.
 90. Mc Loughlin MJ, Mc Loughlin S. Diastolic retrograde arterial flow and biphasic abdominal aortic Doppler wave pattern: an early sign of arterial wall deterioration? *Ultrasound in medicine & biology*. 2013 Apr;39(4):592-6.
 91. Credeur DP, Dobrosielski DA, Arce-Esquivel AA, et al. Brachial artery retrograde flow increases with age: relationship to physical function. *Eur J Appl Physiol*. 2009 Sep;107(2):219-25.
 92. Najmeh S, Cools-Lartigue J, Giannias B, et al. Simplified Human Neutrophil Extracellular Traps (NETs) Isolation and Handling. *J Vis Exp*. 2015 Apr 16(98):e52687-93.

- 
93. Swethakumar B, NaveenKumar SK, Girish KS, et al. The action of *Echis carinatus* and *Naja naja* venoms on human neutrophils; an emphasis on NETosis. *Biochim Biophys Acta Gen Subj*. 2020 Jun;1864(6):129561-73.
94. Stackowicz J, Balbino B, Todorova B, et al. Evidence that neutrophils do not promote *Echis carinatus* venom-induced tissue destruction. *Nature communications*. 2018 Jun 13;9(1):2304-7.
95. Chiou JT, Wang LJ, Lee YC, et al. *Naja atra* Cardiotoxin 1 Induces the FasL/Fas Death Pathway in Human Leukemia Cells. *Cells*. 2021 Aug 12;10(8):2073-88.
96. Jiang WJ, Liang YX, Han LP, et al. Purification and characterization of a novel antinociceptive toxin from Cobra venom (*Naja naja atra*). *Toxicon : official journal of the International Society on Toxinology*. 2008 Oct;52(5):638-46.
97. Sun JJ, Walker MJ. Actions of cardiotoxins from the southern Chinese cobra (*Naja naja atra*) on rat cardiac tissue. *Toxicon : official journal of the International Society on Toxinology*. 1986;24(3):233-45.
98. Rochat H, Gregoire J, Martin-Moutot N, et al. Purification of animal neurotoxins: isolation and characterization of three neurotoxins from the venom of *Naja nigricollis mossambica peters*. *FEBS Lett*. 1974 Jun 15;42(3):335-9.
99. Petras D, Sanz L, Segura A, et al. Snake venomomics of African spitting cobras: toxin composition and assessment of congeneric cross-reactivity of the pan-African EchiTAB-Plus-ICP antivenom by antivenomics and neutralization approaches. *J Proteome Res*. 2011 Mar 4;10(3):1266-80.
100. Jiang W-j, Liang Y-x, Han L-p, et al. Purification and characterization of a novel antinociceptive toxin from Cobra venom (*Naja naja atra*). *Toxicon : official journal of the International Society on Toxinology*. 2008 2008/10/01;52(5):638-646.

- 
101. Donnelly-Roberts DL, Lentz TL. Synthetic peptides of neurotoxins and rabies virus glycoprotein behave as antagonists in a functional assay for the acetylcholine receptor. *Pept Res.* 1989 May-Jun;2(3):221-6.
 102. Afifiyan F, Armugam A, Tan CH, et al. Postsynaptic alpha-neurotoxin gene of the spitting cobra, *Naja naja sputatrix*: structure, organization, and phylogenetic analysis. *Genome Res.* 1999;9(3):259-266.
 103. THALLAMPURANAM KRISHNASWAMY SURESH KUMAR, SHUNMUGIAH THEVAR KARUTHA PANDIAN, GURUNATHAN JAYARAMAN, et al. Understanding the Structure, Function and Folding of Cobra Toxins. *Proceedings of the National Science Council, Republic of China.* 1999;23(1):1-19.
 104. Sala A, Cabassi CS, Santospirito D, et al. Novel *Naja atra* cardiotoxin 1 (CTX-1) derived antimicrobial peptides with broad spectrum activity. *PLoS One.* 2018;13(1):e0190778-800.
 105. Gutierrez JM, Lomonte B. Phospholipases A₂: unveiling the secrets of a functionally versatile group of snake venom toxins. *Toxicon : official journal of the International Society on Toxinology.* 2013 Feb;62:27-39.
 106. Singh SB, Armugam A, Kini RM, et al. Phospholipase A₂ with platelet aggregation inhibitor activity from *Austrelaps superbis* venom: protein purification and cDNA cloning. *Arch Biochem Biophys.* 2000 Mar 15;375(2):289-303.
 107. Condrea E, Barzilay M, Mager J. Role of cobra venom direct lytic factor and Ca²⁺ in promoting the activity of snake venom phospholipase A. *Biochim Biophys Acta.* 1970 Jun 9;210(1):65-73.
 108. Helden DFV, Dosen PJ, O'Leary MA, et al. Two pathways for venom toxin

- entry consequent to injection of an Australian elapid snake venom. *Sci Rep*. 2019 Jun 13;9(1):8595-605.
109. Chieh-Fan C, Tzeng-Jih L, Wen-Chi H, et al. Appropriate antivenom doses for six types of envenomations caused by snakes in taiwan. *Journal of Venomous Animals and Toxins including Tropical Diseases*. 2009;15:479-90.
110. 劉健信*、李佳蓉、李蓉、許靜倫、陳昭宏、張筱琦、謝文欽. 蛇毒蛋白應用研究及抗蛇毒血清製造技術 [original]. 疫情報導. 2015 年 2 月 24 日 第 31 卷 第 4 期 2015 年 2 月 24 日 第 31 卷 第 4 期;31(4):76-86.
111. Mao YC, Liu PY, Chiang LC, et al. *Bungarus multicinctus multicinctus* Snakebite in Taiwan. *The American journal of tropical medicine and hygiene*. 2017 Jun;96(6):1497-1504.
112. Su HY, Huang SW, Mao YC, et al. Clinical and laboratory features distinguishing between *Deinagkistrodon acutus* and *Daboia siamensis* envenomation. *The journal of venomous animals and toxins including tropical diseases*. 2018;24:43-51.
113. Chiang LC, Tsai WJ, Liu PY, et al. Envenomation by *Trimeresurus stejnegeri* *stejnegeri*: clinical manifestations, treatment and associated factors for wound necrosis. *The journal of venomous animals and toxins including tropical diseases*. 2020 Sep 18;26:e20200043-55.
114. Liu CC, You CH, Wang PJ, et al. Analysis of the efficacy of Taiwanese freeze-dried neurotoxic antivenom against *Naja kaouthia*, *Naja siamensis* and *Ophiophagus hannah* through proteomics and animal model approaches. *PLoS neglected tropical diseases*. 2017 Dec;11(12):e0006138-58.
115. Lewin M, Samuel S, Merkel J, et al. Varespladib (LY315920) Appears to Be a

- 
- Potent, Broad-Spectrum, Inhibitor of Snake Venom Phospholipase A2 and a Possible Pre-Referral Treatment for Envenomation. *Toxins*. 2016;8(9):248-64.
116. Ownby CL, Colberg TR, Claypool PL, et al. In vivo test of the ability of antiserum to myotoxin a from prairie rattlesnake (*Crotalus viridis viridis*) venom to neutralize local myonecrosis induced by myotoxin a and homologous crude venom. *Toxicon : official journal of the International Society on Toxinology*. 1984;22(1):99-105.
117. Leão-Torres AG, Pires CV, Ribelato AC, et al. Protective action of N-acetyl-L-cysteine associated with a polyvalent antivenom on the envenomation induced by *Lachesis muta muta* (South American bushmaster) in rats. *Toxicon : official journal of the International Society on Toxinology*. 2021 Jul 30;198:36-47.
118. Rudresha GV, Urs AP, Manjuprasanna VN, et al. Echis carinatus snake venom metalloprotease-induced toxicities in mice: Therapeutic intervention by a repurposed drug, Tetraethyl thiuram disulfide (Disulfiram). *PLoS neglected tropical diseases*. 2021 Feb;15(2):e0008596-620.
119. Snakes of Taiwan [Internet]. Matthew Clarke: Hans Breuer & William Christopher Murphy. 2021. Available from:
https://www.snakesoftaiwan.com/home_zh.html.

This document certifies that the manuscript

Approach for the mechanism of Naja atra snakebite-related dermonecrosis

prepared by the authors

Cheng-Hsuan Ho

was edited for proper English language, grammar, punctuation, spelling, and overall style by one or more of the highly qualified native English speaking editors at AJE.

This certificate was issued on **November 18, 2021** and may be verified on the [AJE website](https://aje.com) using the verification code **616D-A248-225A-841E-E4AA**.



Neither the research content nor the authors' intentions were altered in any way during the editing process. Documents receiving this certification should be English-ready for publication; however, the author has the ability to accept or reject our suggestions and changes. To verify the final AJE edited version, please visit our verification page at aje.com/certificate. If you have any questions or concerns about this edited document, please contact AJE at support@aje.com.